ARF

ARMOUR RESEARCH FOUNDATION OF ILLINOIS INSTITUTE OF TECHNOLOGY

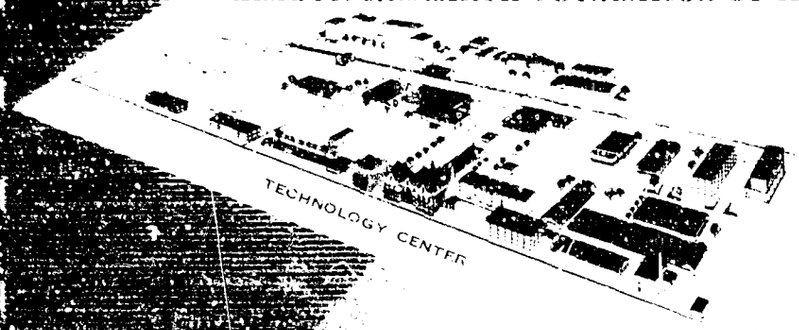

REVISION OF STANDARDS FOR ATTENUATION MEASUREMENTS OF SHIELDED ENCLOSURES

Third Quarterly Progress Report
1 January 1959 - 31 March 1959
Contract No. NObsr-72824
ARF Project No. 2108

For:

Bureau of Ships
Department of the Navy
Washington 25, D. C.

April 1959

ARMOUR RESEARCH FOUNDATION
of
Illinois Institute of Technology
Technology Center
Chicago 16, Illinois

REVISION OF STANDARDS FOR ATTENUATION MEASUREMENTS OF SHIELDED ENCLOSURES

Third Quarterly Progress Report
1 January 1959 - 31 March 1959
Contract No. NObsr-72824
ARF Project No. E108

For:
Bureau of Ships
Department of the Navy
Washington 25, D. C.

Copy No. 18

REVISION OF STANDARDS FOR ATTENUATION MEASUREMENTS OF SHIELDED ENCLOSURES

ABSTRACT

This report covers the work performed during the third quarter of a one-year research program which began on 18 June 1958. The program consists of theoretical and experimental investigations leading to an improved standard for testing shielded enclosures in the frequency range of 14 kilocycles to 10,000 megacycles. The improved standard is being formulated in terms of tests at approximately 14 kilocycles, in the neighborhood of the resonant frequencies of the room, and at 10,000 megacycles. The reasons for choosing these frequencies are; (1) shielding against low-frequency, low-impedance fields is difficult compared to other types of fields, (2) at the mid-frequencies, enclosures exhibit resonances which can significantly affect the performance of the room, and (3) at very high frequencies shielded enclosures exhibit phenomena not predictable from their performance at the lower frequencies.

Two methods for evaluating shielded enclosures using low-impedance, low-frequency fields are under investigation. The first involves the use of a large rectangular loop which surrounds and "immerses" the room in an essentially magnetic field. An average value of the field penetrating the room is obtained using a twelve-inch pick-up loop in the center of the room, and a two-inch pick-up loop is used to explore the field in the neighborhood of wall and door joints. Results indicate that a single imperfect joint will measurably affect the average field in the center of the room,

while the particular joint causing trouble can be located using the small loop.

The shielding effectiveness of a room can also be measured using two 12-inch co-planar loops placed on either side of a wall, one loop acting as a source and the other as a sensor. Tests indicate that measurements made on one wall are insensitive to imperfect joints on another. This is in contrast to the large loop test in which the field in the center of the room is sensitive to poor joints in various parts of the room.

Measurements of the shielding effectiveness of materials using two small loops indicate that the inverse frequency law which gives the reduction of coupling between two coaxial loops due to a sheet conductor inserted between them is not satisfactory. The test results are more accurately fitted by a negative exponential law in which the exponent is proportional to the thickness of the sheet and to the square root of the frequency.

A shielded enclosure is a rectangular cavity capable of exhibiting resonances. Because of this, a condition can exist in which a very high electric field intensity can be present in the interior of the room, due to outside sources, even though the electric field at the surface of the inner walls (the field penetrating the enclosure) is small. This may cause the "effective" attenuation of the room to be reduced significantly at resonance. Measurements of the resonant frequencies of the room agree very well with predicted values and high Q's (of the order of 500) have been observed. Electromagnetic field absorbers placed inside the enclosure have demonstrated the ability to reduce the effect of resonances.

A measurement of field intensity inside of a shielded enclosure in the neighborhood of its resonant frequencies may be made using a dipole antenna. Measurements have demonstrated that, unless the dipole is

electrically short (of the order of $\lambda/8$), its impedance will be different depending upon whether the antenna is located inside or outside the enclosure. Consequently, the electrical length of a dipole probe should be kept short so that the antenna will remain matched to the measuring device whether it is used inside or outside of the enclosure.

In the kilomegacycle region, the penetration of an electromagnetic field through screen materials takes place because of the perforations in the material. This phenomenon has been examined theoretically by H. Bethe, the result being the dipole theory of hole penetration. The theory is developed for holes in a conducting sheet and its applicability to screen materials remains to be demonstrated.

The testing of the enclosure in the neighborhood of 10 kilomegacycles has been initiated using an AN/APS-25 radar and an AN/URM-17 Radio Interference-Field Intensity Measuring Set. The test results obtained to date are not complete and the attenuation of 80 db obtained for a doubly screened enclosure (of cell-type construction) can only be considered as representative. Tests have also been made to obtain information regarding the reaction of the enclosure wall on the source. This was done by measuring the reflected wave in a waveguide, one end of which was connected to a 10 kilomegacycle source and the other to a horn illuminating the wall of the enclosure. The reflection coefficient was measured as a function of the distance of the horn from the wall.

A coaxial device is under development for evaluating the shielding effectiveness of materials to plane waves. Until recently, difficulty has been experienced in removing the effects of contact resistance; however, immediately prior to the writing of this report, the unit was modified and initial

measurements indicate that this problem has been rectified. The device has been analyzed from the view-point of electromagnetic field theory, transmission line theory, and circuit theory. Expressions are obtained for reflection and attenuation losses.

TABLE OF CONTENTS

TABLE OF CONTENTS (Cont'd)

LIST OF FIGURES

LIST OF FIGURES (Cont'd)

REVISION OF STANDARDS FOR ATTENUATION MEASUREMENTS OF SHIELDED ENCLOSURES

I. PURPOSE

The purpose of this research is to develop improved techniques for measuring the effectiveness of shielded enclosures in the frequency range of 14 kilocycles to 10,000 megacycles per second and to provide recommendations for standard methods of evaluating such enclosures.

II. GENERAL FACTUAL DATA

A. Identification of Personnel

Name	Title	Man-Hours To End of 2nd Quarter	Man-Hours Total
R. B. Schulz	Research Engineer-Project Engineer	188	431
L. C. Peach	Research Engineer	443	803
D. P. Kanellakos	Assistant Engineer	0	484
L. J. Greenstein	Technical Assistant	96	136
Additional Engineering Services		0	41

B. References

(1) "Electromagnetic Fields", Vol. I, E. Weber, John Wiley and Sons, Inc. New York, 1950, (pp. 131-134).

(2) "Static and Dynamic Electricity", W. R. Smythe, McGraw-Hill Book Co., Inc., 1950.

(3) "Theory, Design and Engineering Evaluation of Radio-Frequency Shielded Rooms", C. S. Vasaka, Report No. NADC-E4-S4129, U. S. Naval Air Development Center, Johnsville, Pennsylvania, 1956.

(4) "Theory of Diffraction by Small Holes", H. A. Bethe, The Phys. Rev., 66, Oct. 1944.

(5) "Principles of Microwave Circuits", Montgomery, R. H. Dicke, and E. M. Purcel, MIT Radiation Laboratory Series, Vol. 8, McGraw-Hill Book Co., Inc., 1948.

(6) "Microwave Antenna Theory and Design", S. Silver, MIT Radiation Laboratory Series, Vol. 12, McGraw-Hill Book Co., Inc., 1949.

C. Meetings and Conferences

Date: February 3-4, 1959

Place: Armour Research Foundation

Personnel Attending:

Mr. A. P. Massey, Bureau of Ships

Mr. M. Epstein, Armour Research Foundation

Mr. L. J. Greenstein, Armour Research Foundation

Mr. D. P. Kanellakos, Armour Research Foundation

Mr. L. C. Peach, Armour Research Foundation

Mr. R. B. Schulz, Armour Research Foundation

Personnel of Armour Research Foundation reviewed the progress on the project with Mr. Massey. The work to be conducted in the third quarterly interval was also discussed.

III DETAILED FACTUAL DATA

A. Introduction

The purpose of this program of research is to provide a specification for testing shielded enclosures which will furnish a maximum amount of information regarding the enclosure, without requiring an undue amount of equipment or effort.

At the present time it is believed that tests should be performed in three frequency ranges, in the neighborhood of 14 kilocycles, at or near the resonant frequencies of the room, and at 10 kilomegacycles. The reasons for selecting these frequency ranges will be given in detail in subsequent sections of this report. Briefly, at low frequencies shielding against low-impedance fields is much more difficult than other types of fields and, consequently, a test using such fields is believed to be necessary. Enclosures exhibit resonance phenomena which can very significantly affect the performance of the room; a test in this frequency range is therefore suggested. At the very high frequencies, shielded enclosures exhibit behavior not predictable from their performance at lower frequencies and, consequently, a test at these frequencies is advisable. A discussion of the tests performed in the three frequency ranges is contained in Sections III-B, -C, and -D respectively.

The performance of a shielded enclosure is largely determined by both the construction of the room and the wall materials. A coaxial device for testing shielded-enclosure materials was discussed in the previous quarterly progress report. A more complete discussion of the device is given in Section III-E. The primary problem involved in the development of the device has been the need for minimization of contact resistance between the

coaxial holder and the test sample. A means for circumventing this problem is under investigation and is also discussed in Section III-E.

B. Low-Frequency Tests

1. Introduction

Since the presence of low-impedance fields at low-frequencies is quite common, the shielding effectiveness of a shielded enclosure should be measured against low-impedance magnetic fields. These low-impedance fields can most easily be produced by current loops whose dimensions are small compared to the wavelength.

2. Low Impedance Fields

One of the methods used to produce low-impedance magnetic fields for testing the shielded enclosure utilizes a large, square loop completely surrounding the shielded enclosure. The loop to enclosure separation is four inches. When a moderate current flows in the turns of the loop, it produces a sufficiently strong magnetic field which completely surrounds all sides of the shielded enclosure. This arrangement allows measurements on the overall performance of the shielded enclosure to be made with simplicity.

3. Experimental Results

The large rectangular loop consists of 10 turns of No. 18 plastic insulated wire with a d.c. resistance of 2.6 ohms. It completely surrounds the copper-screened, cell-type shielded enclosure* of approximate dimensions 8 feet x 10 feet x 8 feet. Measurements of the input impedance of the

---

* Supplied by Ace Engineering and Machine Company, Inc. Philadelphia, Pennsylvania

loop were made with a General Radio Impedance Bridge at 200 kc with the loop in a horizontal plane midway down the screen room. The impedance value recorded was 25 + j 1450 ohms. In order to obtain a sufficiently large value of current flowing in the loop, so that measurable fields will be produced inside the shielded enclosure, the inductance was tuned out at 200 kc. using a 480-uuf capacitor. The inductance of the loop is therefore 1.15 mh and 1.32 mh when calculated from the impedance and capacitance measurements, respectively. The variation of magnetic field intensity detected inside the shielded enclosure, with respect to voltage applied to the loop terminals, was linear. Both magnetic and electric fields can be detected inside the screen room by the use of a loop and a whip (rod) antenna, respectively.

a. Insertion-Loss Measurements

The large rectangular loop was used in conjunction with a small twelve-inch circular ten turn loop in making insertion-loss measurements. The voltage induced in the ten turn loop at the center of the room, while the large loop was excited, was compared with the theoretically expected voltage induced in the loop in the absence of the enclosure. Both measurements are taken in the center and plane of the loop. In addition the insertion loss was measured using two co-planar loops[1]. Measurements were performed at 15 kc. and 200 kc.

---

1 Attenuation measurements for low impedance magnetic fields are usually made with two twelve inch in diameter, single turn loops placed a distance of twenty five inches apart. The coupling of the loops is measured with and without the presence of a screening material. See MIL-STD-285 p. 5.

		Insertion Loss at	
		15 k	200 kc
1.	Large loop outside: Small 12-inch, 10 turn loop inside at the center of the room.	61 db	97 db
2.	Two 12-inch 10 turn loops; 7 inches apart	56 db	95 db
3.	Two 12 inch single turn loops; 7 inches apart	56 db	---

In the two-small-loop method the two loops were placed seven inches apart to obtain adequate coupling between them. The insertion loss measured under the conditions 1 and 2 or 3 above is not the same because the impedance of the fields produced by the one foot loop and the large loop is different and, also, because the loop and shielding geometry is not the same. The coupling between the two 12 inch single turn loops at 200 kc. was too weak to give measurable signals; thus no value of insertion loss is given at 200 kc. for these loops.

The theoretically expected value of the voltage induced in a small single-turn circular loop when placed in the center and co-planar with a large rectangular loop was obtained from the following.

Consider a rectangular loop in the xy-plane of side 2a and 2b meters, as shown in Figure 1, carrying a current I amperes in its conductor whose cross section is considered small compared with 2a or 2b. The vector potential at a distance r_s from an element of a conductor of length $d\ell_s$ carrying a current I is given by

$$(1) \quad A = \frac{\mu I}{4\pi} \oint \frac{d\ell_s}{r_s}$$

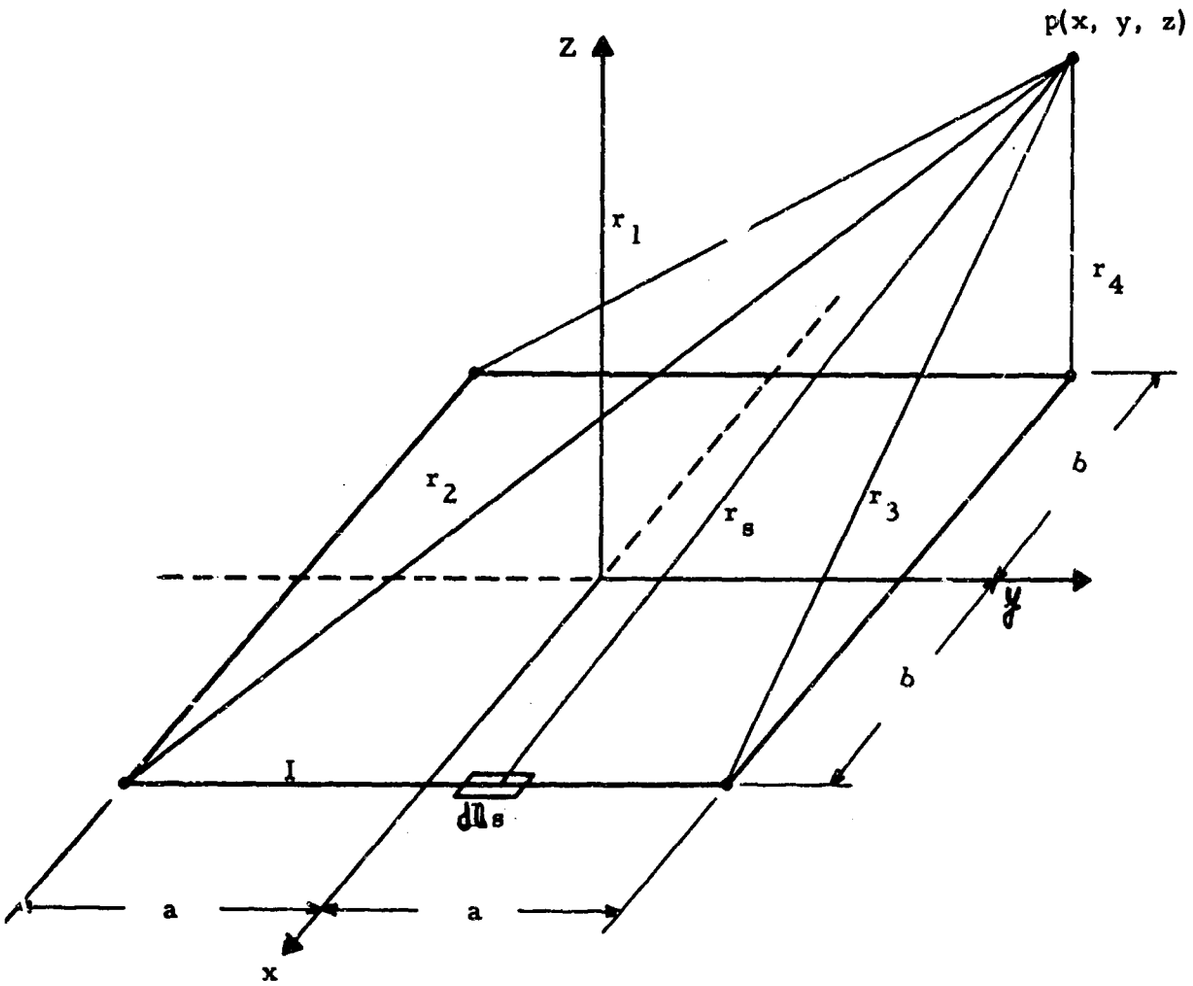

FIG. 1 - FIELD DUE TO A RECTANGULAR LOOP

For the rectangular loops, A has two components A_x and A_y given by[1]

$$(2)\quad A_x = \frac{\mu I}{4\pi} \ln\left[\left(\frac{r_1 + a + x}{r_2 - a + x}\right)\left(\frac{r_3 - a + x}{r_4 + a + x}\right)\right]$$

$$(3)\quad A_y = \frac{\mu I}{4\pi} \ln\left[\left(\frac{r_2 + b + y}{r_3 - b + y}\right)\left(\frac{r_4 - b + y}{r_1 + b + y}\right)\right]$$

where r_1, r_2, r_3, r_4 are the distances from the point P to the individual vertices of the rectangular loop, respectively. At the xy plane of the rectangle, $B_x = B_y = 0$.

The flux density in the plane of the loop is given by

$$(4)\quad B_z = \frac{\partial}{\partial x} A_y - \frac{\partial}{\partial y} A_x = \frac{\mu I}{4\pi} \sum_{n=1}^{4} (-1)^n \frac{x_n + y_n - r_n}{x_n y_n}$$

Eq. (4) is completely general on the xy plane ($z = 0$.)

The field at the center of the loop is given by

$$(5)\quad B_z = \frac{\mu I}{\pi} \frac{\sqrt{a^2 + b^2}}{ab}$$

The large rectangular loop, ($a = 1.15$ meters , $b = 1.55$ meters) carrying a current of 200 ma. rms will yield a field at the center equal to,

$$(6)\quad B_z = 4.23 \times 10^{-7} \frac{\text{webers}}{\text{meter}^2}$$

---

[1] Reference (1) pp. 131-134.

This field will induce a voltage in a 12-inch single-turn circular loop equal to

$$(7)\quad \mathcal{E} = 2\pi f A B_z = 2.93 \text{ mv at } 15 \text{ kc.}$$

where A is the area of the circular loop.

The large rectangular loop was taken off the screen room and the induced voltage at the center of the loop was experimentally measured. It was found that in the frequency range from 1 to 15 kc., the ratio of measured voltage to the calculated voltage was 0.855 over the frequency band mentioned above. The reasons for this difference have not been determined as yet.

b. Effect of Slit (Leaky Joint) on Shielding Effectiveness

This test was performed in order to find a suitable method of identifying leaky joints at low frequencies. The contact surfaces between the screen door and the door jamb were thoroughly cleaned with emery cloth.

The voltage induced in a ten-turn loop inside the room, due to a field produced by a similar and co-axial loop outside the room was measured. The loops were seven inches apart. This was done at several locations in the room. The large loop was then excited, and the voltage induced in a ten-turn loop inside the room was measured at the same locations.

The entire vertical contact surfaces between the handle side of the door and jamb were covered with adhesive tape to produce an insulated joint. The above measurements were then repeated. The ratio of the induced voltages obtained in the presence and absence of the tape are listed below.

The measurements were made at 12 kc.

(1) Coupling between two 12-inch, 10-turn loops with and without tape.

Door:	$\frac{V_{\text{with tape at joint}}}{V_{\text{without tape at joint}}}$
Handle side of	10
Hinge side of	1.2
Middle panel of	1.2
Side Panels:	
Middle position	1.0

(2) Coupling between large rectangular loop "bathing" the room from outside and a 12-inch, 10 turn loop inside at location indicated.

Door:	$\frac{V_{\text{with tape at joint}}}{V_{\text{without tape at joint}}}$
Handle side of	10
Hinge side of	1
Middle panel of	3
Center of room	8

A small 2-inch diameter, 150-turn loop was used as a search device for locating leaks while the large loop was exciting the room from the outside. When the search loop was carried around the periphery of the room and at the same height as the rectangular loop, it was found that the variation of the pickup voltage was very pronounced near leaky joints. This test revealed that some joints leaked about 5 to 15 times as much as the middle of the panels whereas the taped door was leaking 30 times as much as the center of panels.

Figure 2 depicts a plan view of the relative magnitude of the magnetic field at 12 kc inside the screen room as was picked up by the small searching loop (with no tape at the joint). The pronounced variation of the field intensity near leaky joints is evident. The figure indicates that the joint near the hinge side of the door was leaking excessively. This joint was tightened and the test repeated. As can be seen from Figure 3, the amount of leaking was reduced considerably.

The insertion loss of the shielded enclosure was also measured with the presence of the leaky (taped) joint using the large rectangular loop outside and the small loop inside and at the center of the shielded enclosure. It was found at 12 kc the taped joint reduced the insertion loss by 18 db.

4. Conclusions

As can be seen from test (2), the reading in the center of the room, with the tape at the door joint, is about 8 times as large when the door joint is not leaking. This demonstrates that the test employing the large rectangular loop is sensitive to leaky joints. The leaky joints can be located using a small probe loop to explore the inside of the room while the large loop is excited. Test (1) indicates that the two-loop-method is insensitive to a leaky joint unless the test is made at that joint.

It appears that the large loop method is also a more efficient technique than the two 12-inch loop method. The large loop provides a constant magnetic field around the entire room, hence only one person is required to explore the fields in the room with a small searching loop. The two-loop method requires the services of two people at the same time and greater care must be exercised in keeping the distance between loops constant so that

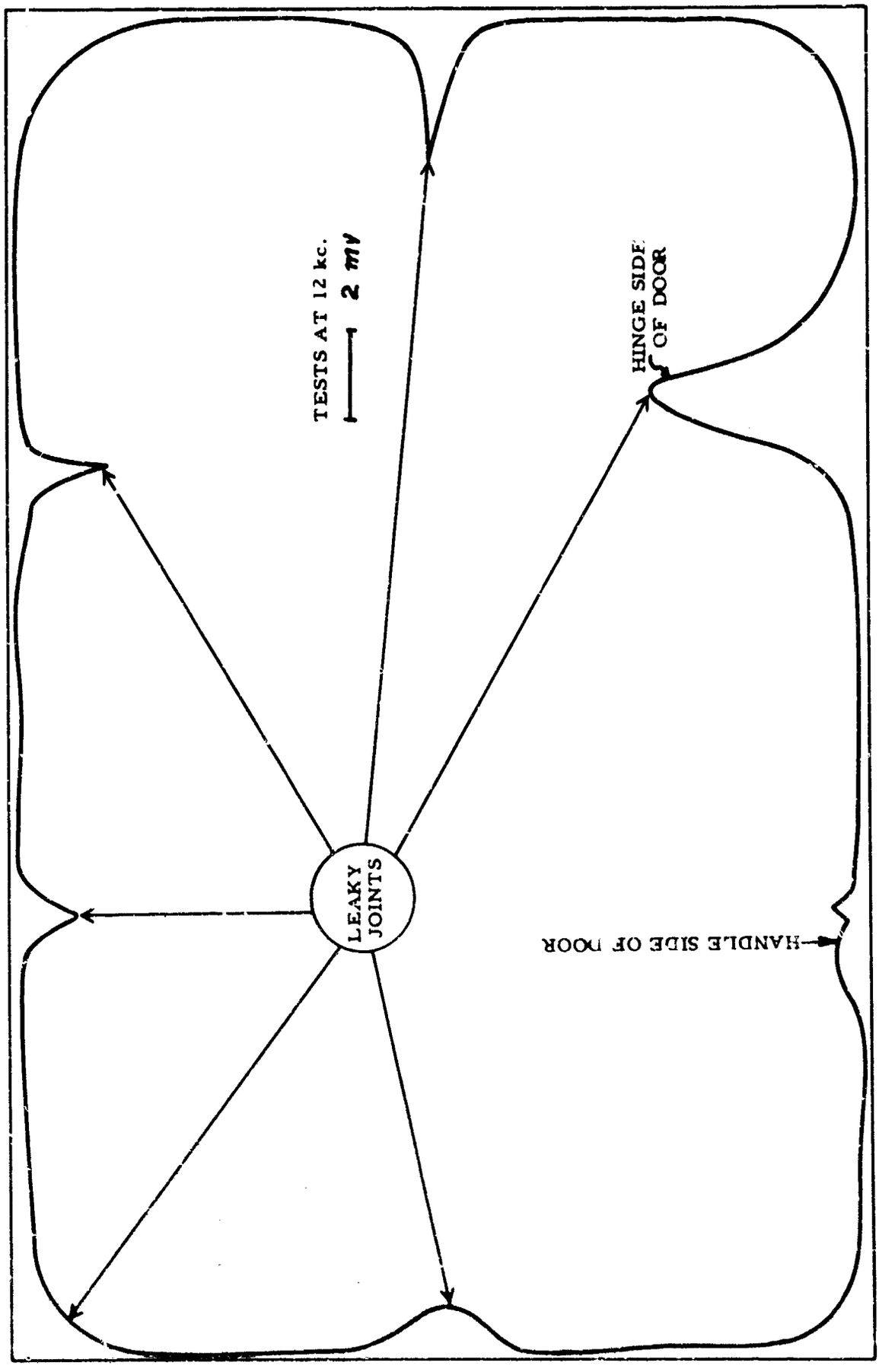

FIG. 2 - PLAN VIEW OF SHIELDED ENCLOSURE SHOWING LEAKY JOINTS

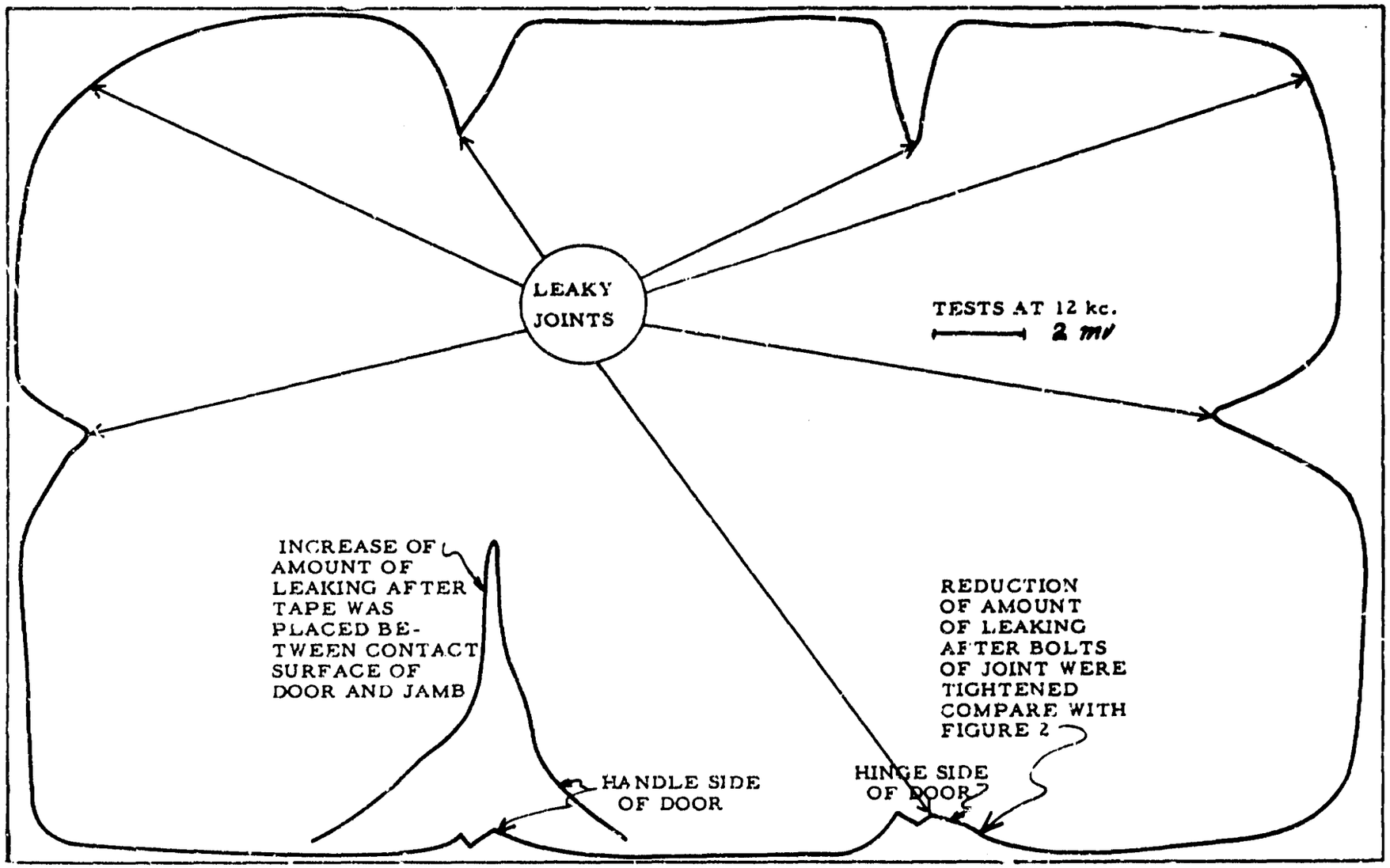

FIG. 3 - PLAN VIEW OF SHIELDED ENCLOSURE SHOWING LEAKY JOINTS

repetitive measurements may be obtained.*

5. Experimental Verification of the Formula for the Coupling Between Two Coaxial Loops

In the Second Quarterly Progress Report, a formula was given for the reduction in the coupling between two coaxial loops due to an infinite planar sheet of conducting material.

$$(8) \quad N = \frac{20.3\, R_r C}{f d \mu_r (a^2+b^2+C^2)}$$

N = ratio of lux linkages with the absence and the presence of the sheet

f = frequency in cycles per second

d = thickness of sheet in inches

a, b = radii of loops in inches

c = distance between loops in inches

R_r = resistivity, relative to copper, of sheet = $\frac{\rho}{\rho_{cu}} = \frac{1}{\sigma \rho_{cu}}$

μ_r = relative permeability of sheet = $\frac{\mu}{\mu_o}$.

The factors in the above equation which characterize the sheet are R_r, d, and μ_r while those which characterize the loops are a and b.

The general formula[1] from which the above equation is derived is

$$(9) \quad A_1 + A_2 = \frac{2R_T}{\mu} \frac{\partial}{\partial z} \int_0^\infty A_1\left(t-\tau, x, y, z-\frac{2R_T}{\mu}\tau\right) d\tau$$

---

* The energy coupled between two loops at close spacings varies inversely as the cube of the distance between their centers. Thus small errors in the spacing of the loops is apt to produce large errors in their coupling.

1 Reference (2), p. 533

where A_1 is the applied vector potential

A_2 is the vector potential resulting from the presence of the sheet

R_T is the surface resistivity of the sheet

μ is the permeability of the sheet

The formula is of interest because it gives the change in vector potential resulting from an infinite planar sheet in terms of an integral of the applied vector potential. Thus, the shielding effectiveness of a sheet of material can be calculated for complex applied fields without resorting to mode solutions.

Equation (8) was investigated for three materials: copper, aluminum, and steel. Tests were performed for sheets of thicknesses of 1/32", 1/16", and 1/8" depending upon availability.

The coaxial loops used consisted of 150 turns wound to a radius of one inch. The current was supplied to the driven loop by an audio oscillator and the voltage induced in the second loop was measured by an audio voltmeter. A frequency range of 100 cycles to 20,000 cycles was covered in the test.

In the test procedure the value of c changed with the thickness of the material, that is, c was related to d by

(10) $c = K + d$

The formula then takes the form

$$(11) \quad N = \frac{R_r \quad (K+d)\,20.3}{d\,\mu_r f\,[a^2+b^2+(K+d)^2]}$$

In the tests, a and b were each one inch and K was 0.69 inch, so that the formula reduces to

$$(12) \qquad N = \frac{R_r}{d\mu_r}\left(\frac{0.69 + d}{2.48 + 1.38d + d^2}\right)\frac{20.3}{f}$$

The largest value of d used was 0.125 inch so that d^2 was at most 0.0156 square inches, which can be neglected compared to 2.48.

The first set of curves, Figures 4 through 6, gives the value of N versus frequency for copper, aluminum, and steel. Both the theoretical curves given by (12) and experimental curves are given.

The regular deviations of the experimental from the theoretical curves indicate that another law may be more representative. The general shape of the curves suggests a law of the form

$$(13) \qquad N = e^{-k\sqrt{f}}$$

Suitable values of k were obtained for a particular sheet (material and thickness) by using the measured values of N, at various frequencies, to calculate values of k corresponding to these frequencies. The average value of these computed values of k was taken as the value of k for the sheet.

This value of k was then used to calculate an attenuation-versus-frequency curve for that sheet. These curves are shown in Figures 7 through 9. As indicated, the correspondence between experiment and the general form given by (13) is better than that given by the formula (8).

In order to pursue the development of a suitable formula, k was plotted against the thickness of the sheet for sheets of the same material. The results are shown in Figure 10. Although the data are inadequate for an accurate prediction, it suggests the form

$$(14) \qquad k = \alpha d + \delta$$

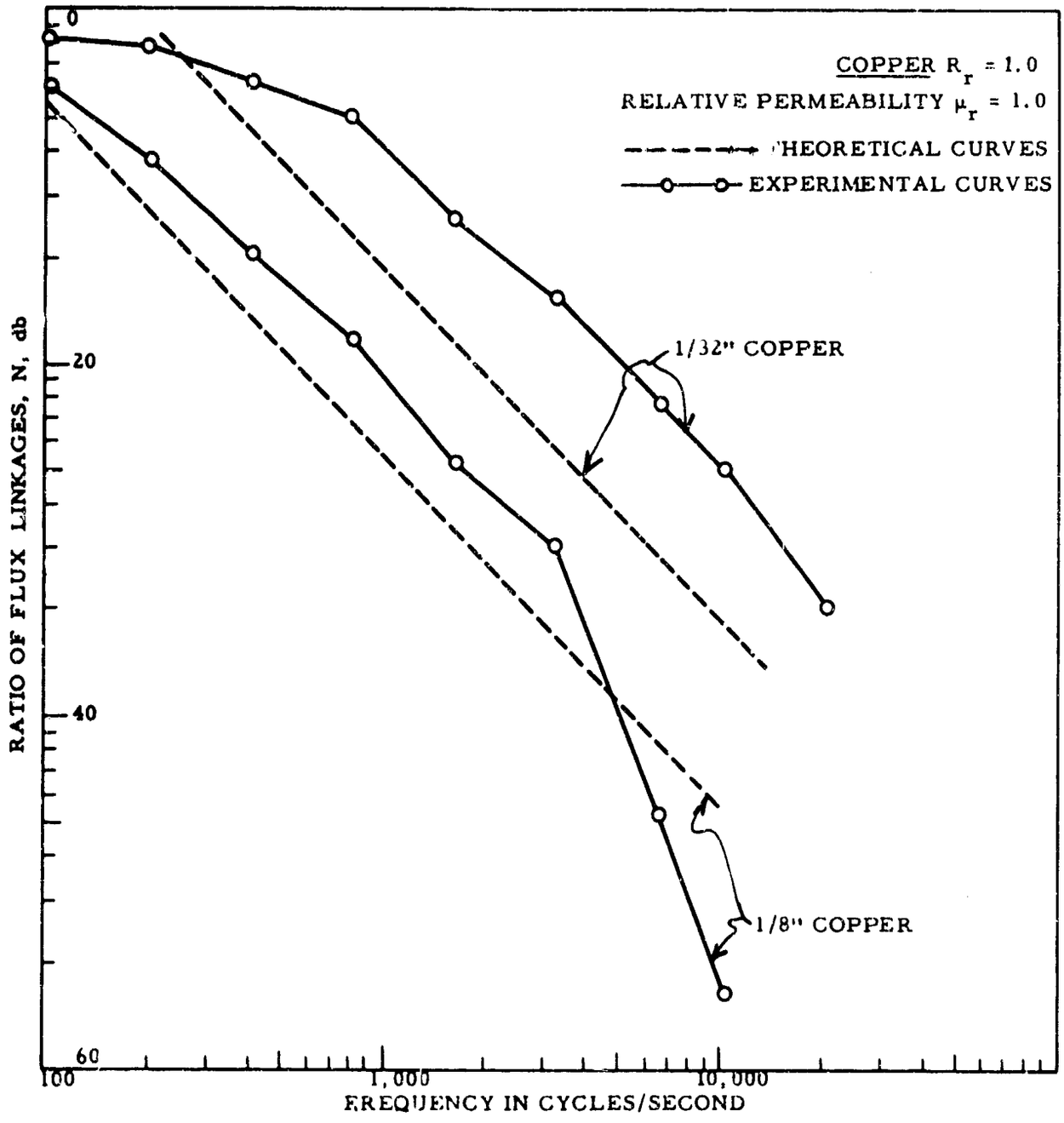

FIG. 4 - TWO-LOOP METHOD OF MEASURING SHIELDING EFFECTIVENESS

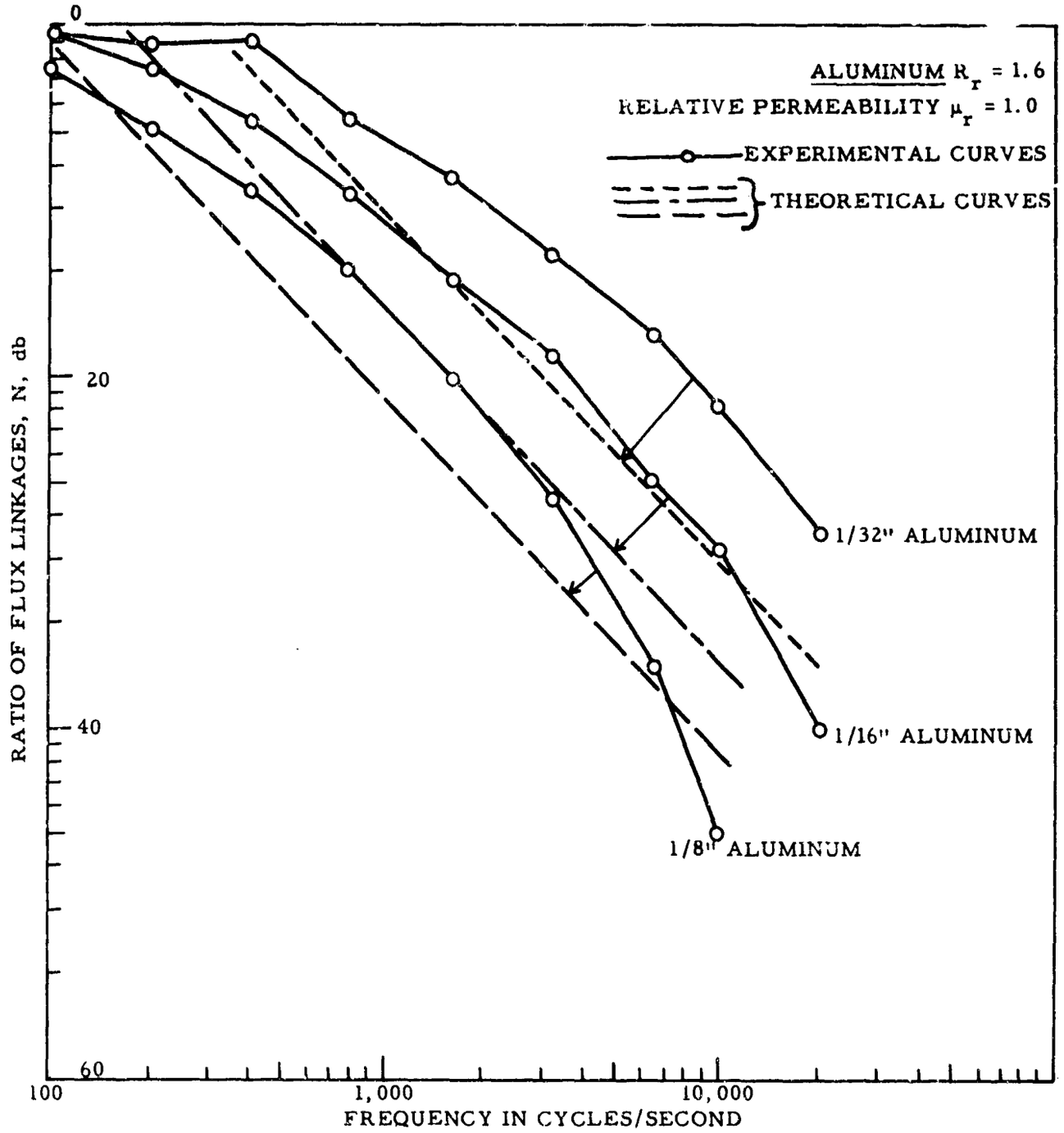

FIG. 5 - TWO-LOOP METHOD OF MEASURING SHIELDING EFFECTIVENESS

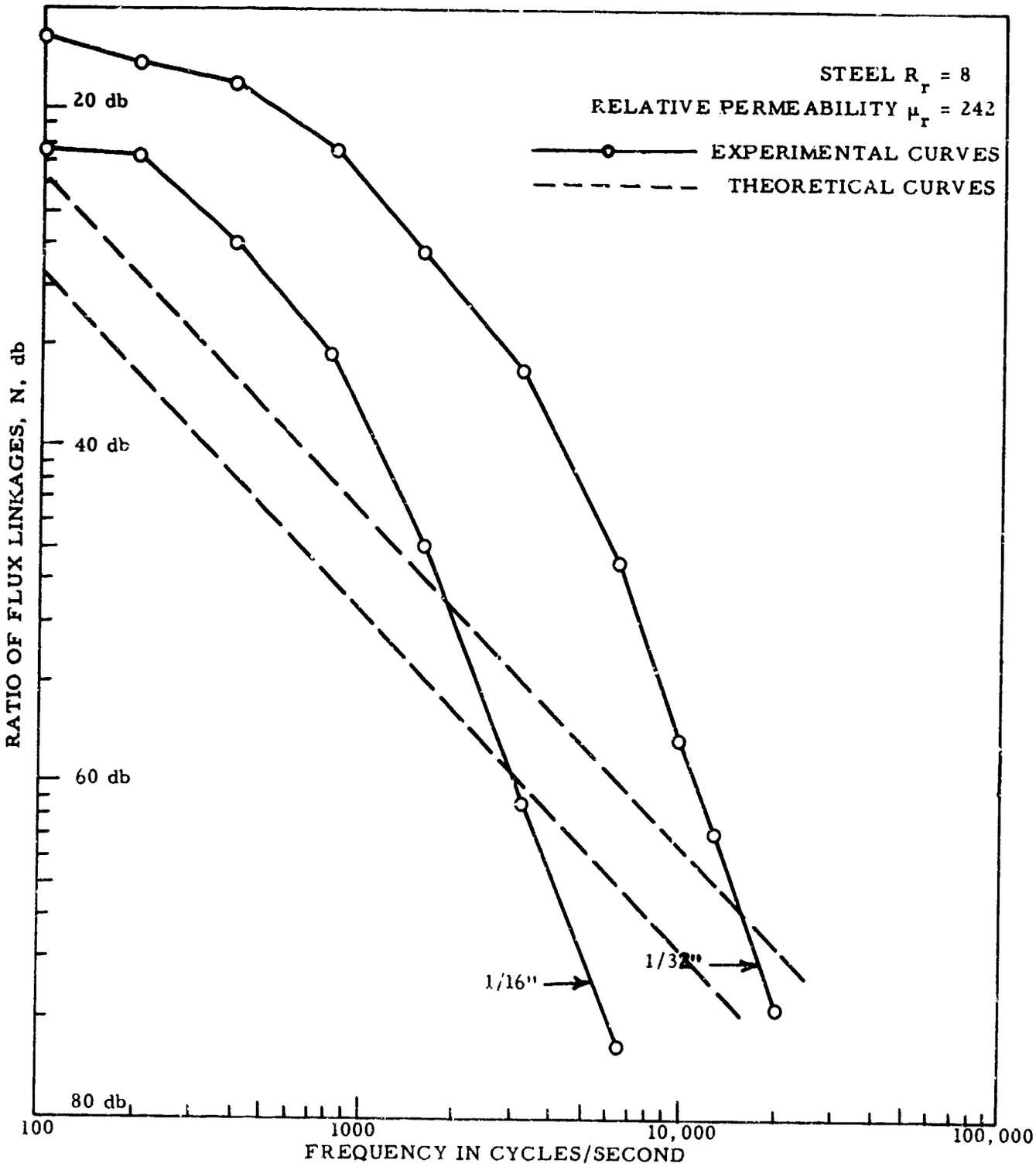

FIG. 6 - TWO-LOOP METHOD OF MEASURING SHIELDING EFFECTIVENESS

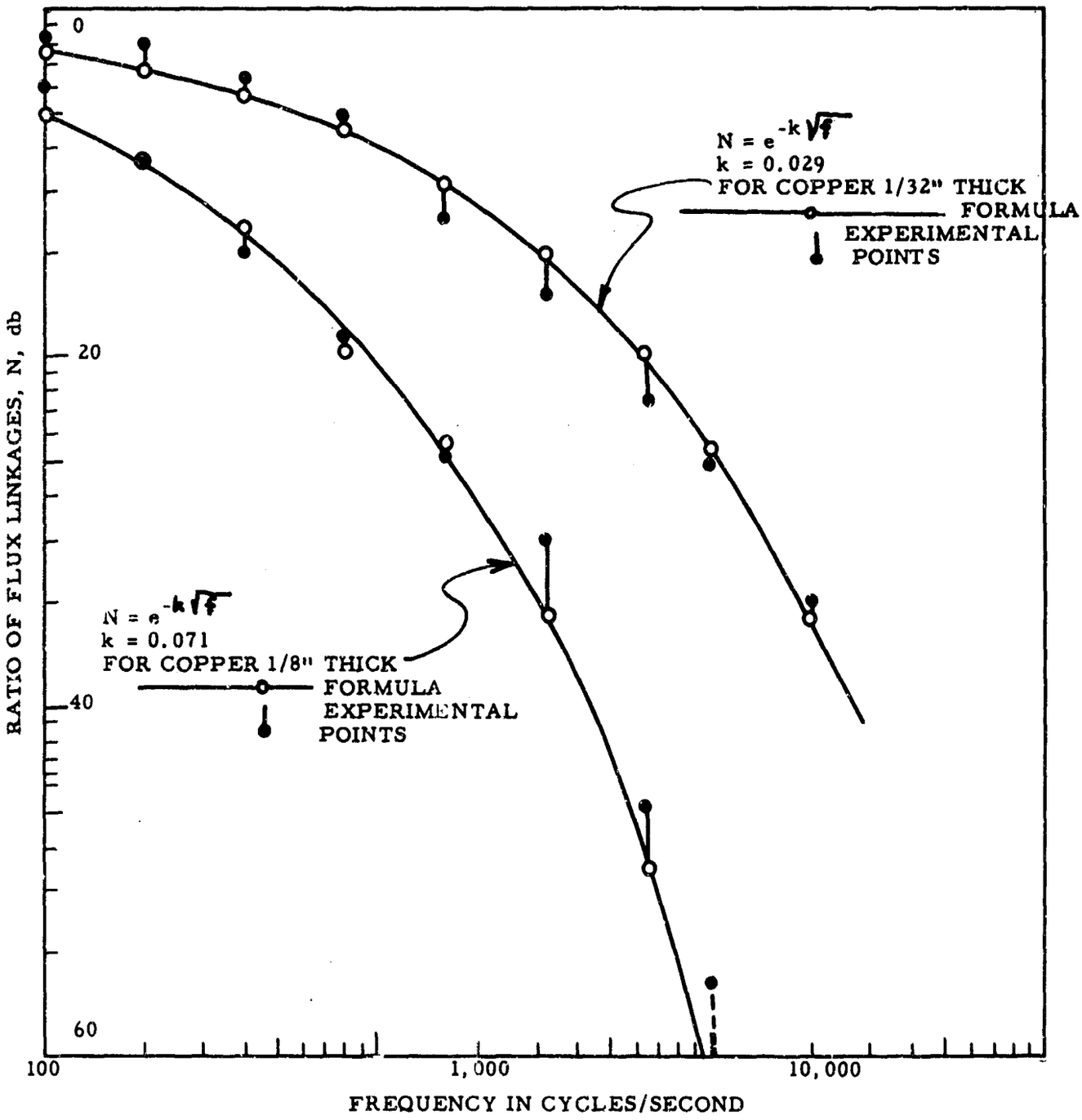

FIG. 7 - EMPERICAL EXPONENTIAL FORMULA FITTING THE DATA OF FIGURE 4

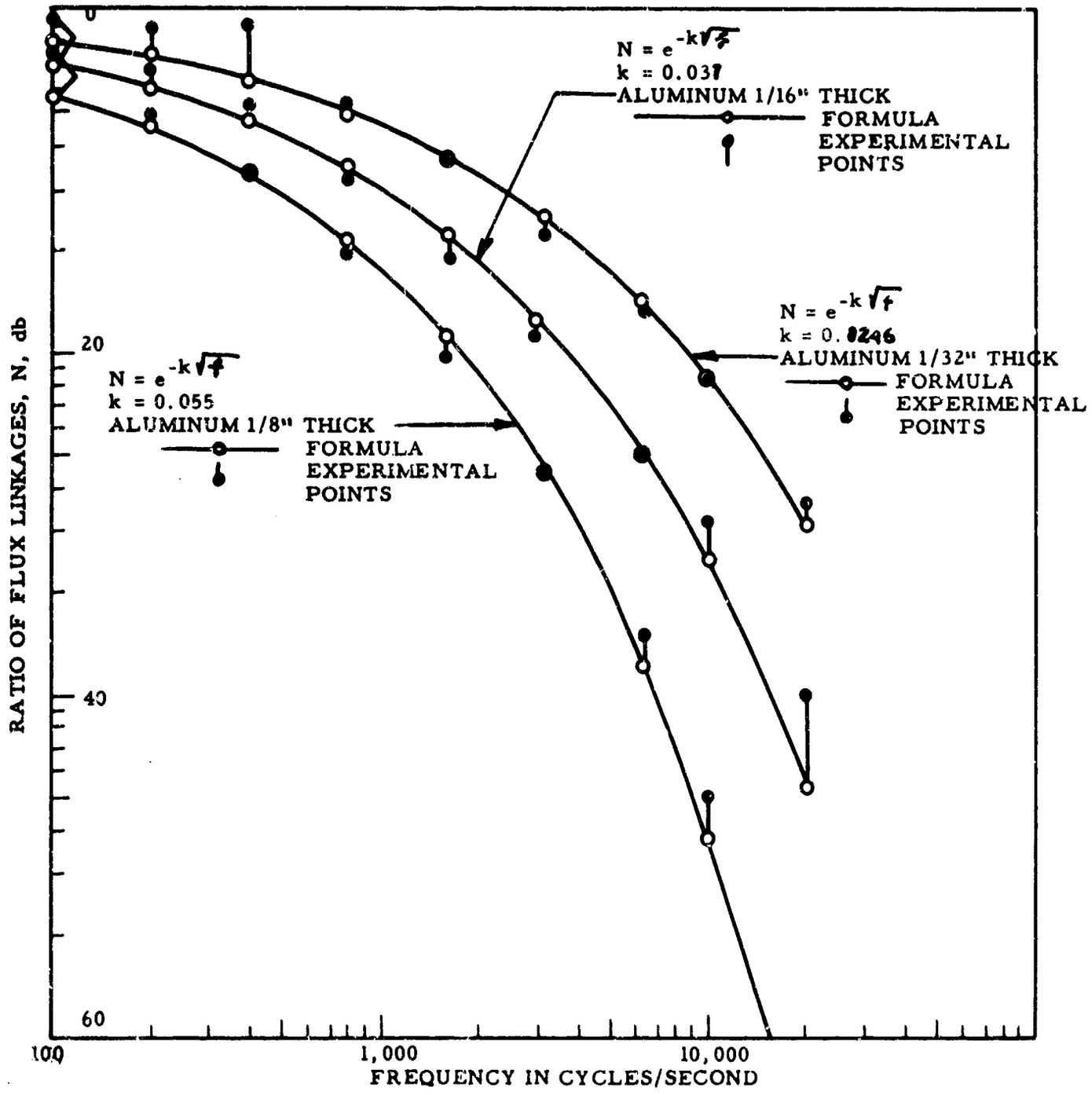

FIG 8 - EMPERICAL EXPONENTIAL FORMULA FITTING THE DATA OF FIGURE 5

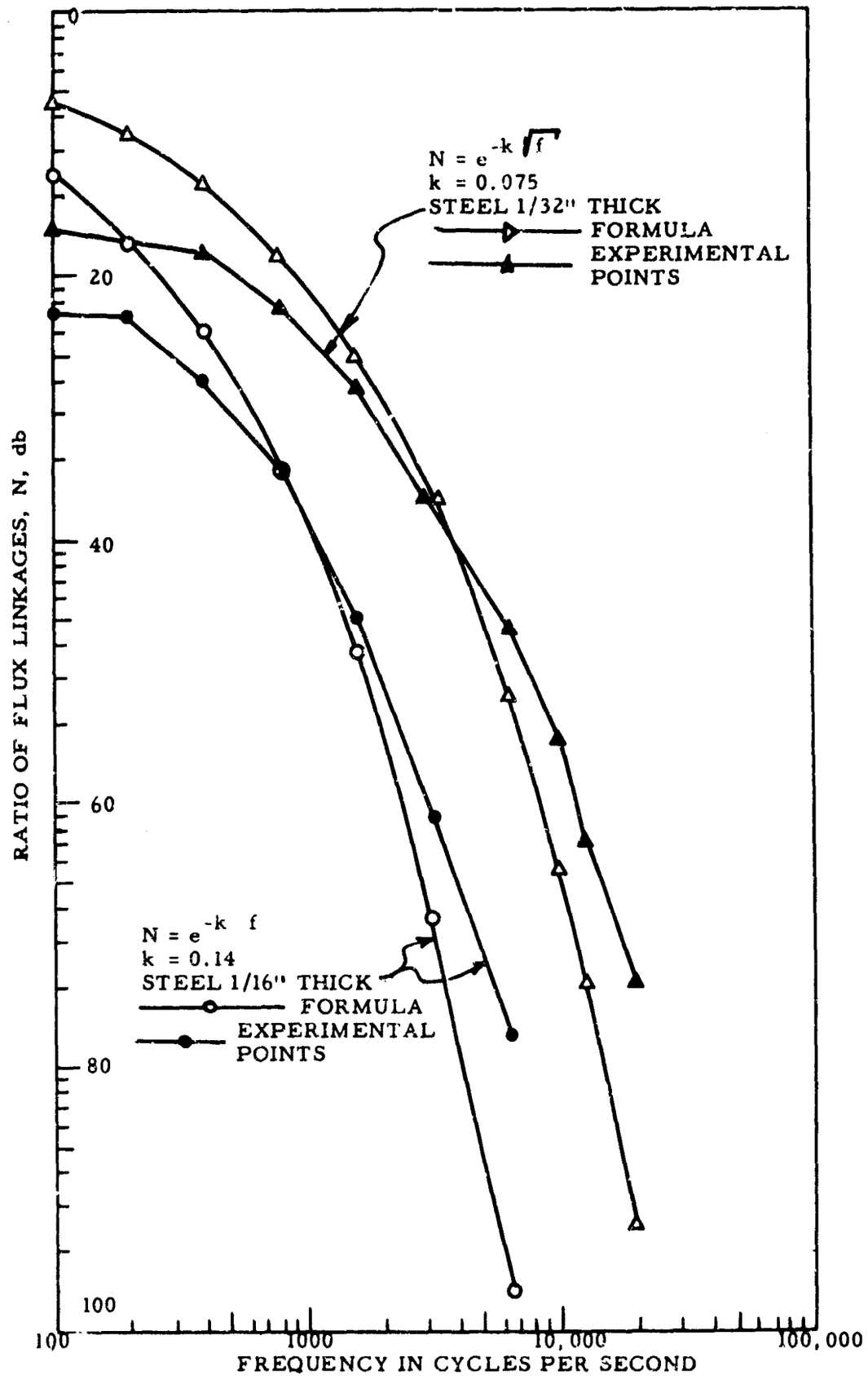

FIG. 9 - EMPERICAL EXPONENTIAL FORMULA FITTING THE DATA OF FIGURE 6

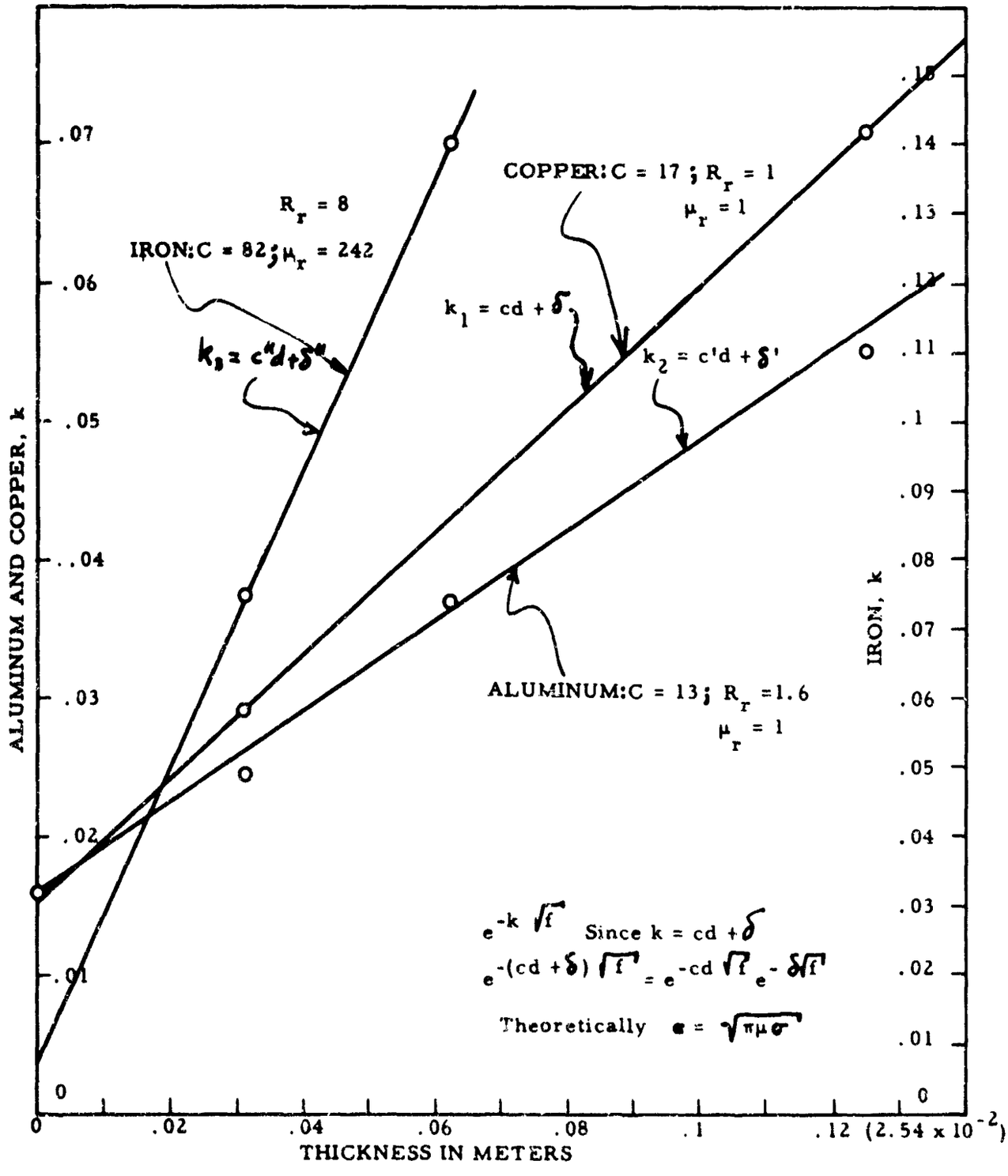

FIG. 10 - GRAPHICAL DETERMINATION OF ATTENUATION CONSTANT

It follows then that (13) will take the form

$$(15)\quad N = e^{-(\alpha'+\delta)\sqrt{f}} = e^{-\alpha d\sqrt{f} - \delta\sqrt{f}}$$

The attenuation of a plane wave passing through a conductor is given by the form

$$(16)\quad e^{-\sqrt{\pi\mu\sigma}\, d\sqrt{f}}$$

where all the symbols in Eq. (16) are defined on page 13 of this report. Equation (16) suggests that the measured value of α should be approximately equal to $\sqrt{\pi\mu\sigma}$. The values of α and $\sqrt{\pi\mu\sigma}$ are given below for copper, aluminum and iron:

Material	α	$\sqrt{\pi\mu\sigma}$
Copper	17	15.1 $\mu_r = 1$
Aluminum	13	12.9 $\mu_r = 1$
Iron (Magnetic)	82	$\sigma_{rdc} = \frac{1}{\rho} \Rightarrow \mu_r = 242$

The data, although inconclusive, suggest that the attenuation is more accurately given by the conventional form of a negative exponential variation than by the hyperbolic variation given by (8).

The discussion, thus far, has been concerned with solid materials. Since a large number of the shielded enclosures are constructed of screening materials, it was of interest to perform tests on these materials. The reduction of flux linkages was measured for two layers of screen material in cell-type construction. The results are shown in Figure 11. Consider again equation (12).

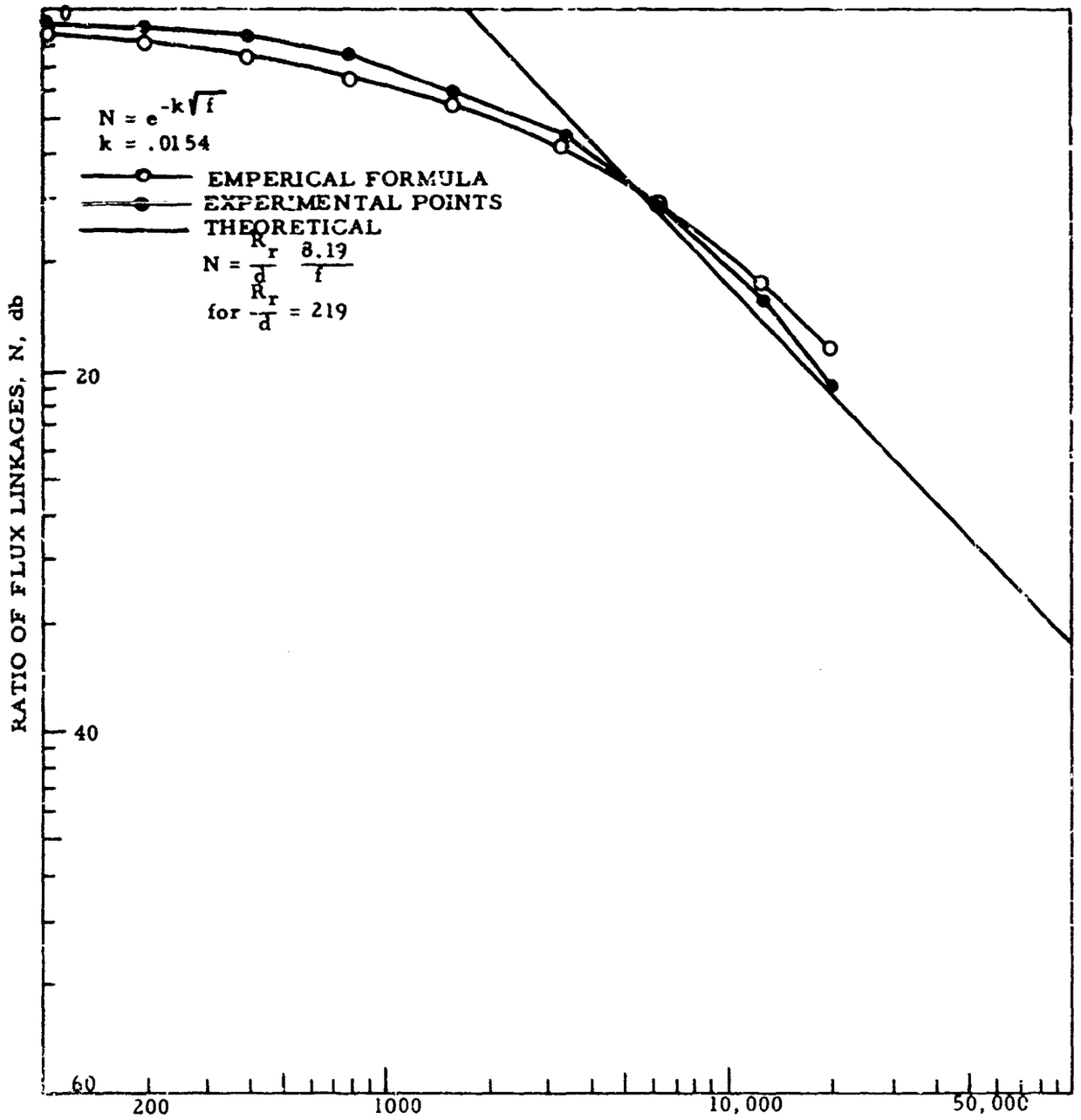

FIG. 11 - ATTENUATION OF DOUBLE-SCREEN COPPER MATERIAL (OXIDIZED)

$$(12)\quad N = \frac{R_r}{d\mu_r}\left(\frac{0.69+d}{2.48+1.38d+d^2}\right)\frac{20.3}{f}$$

For the screen materials, the physical thickness d of the two layers was much less than 0.69 inch so that the formula can be approximately given by

$$(17)\quad N = \frac{R_r\,20.3}{d\mu_r(2.48)f}$$

Since $\mu_r = 1$, it follows that

$$(18)\quad N = \frac{R_r}{d}\frac{8.19}{f}$$

The value of N at f equal to 6400 is 0.28 which yields a value of R_r/d equal to 219. For solid copper to have the same R_r/d ratio would require d to be equal to 0.0046 inch.

The experimental results indicate that the formula given by equation (12) is not at all satisfactory. The selection of $\frac{R_r}{d}$ equal to 219 was arbitrary and would vary with f.

The experimental data were also explored for correspondence to the attenuation formula given by Equation (13),

$$(13)\quad N = e^{-k\sqrt{f}}$$

An averaging process yielded a value of k = 0.0154; this value was then used to plot a curve which is also entered in Figure 11. It is

evident that in the low-frequency region the formula given by equation (13) fits the experimental data much more accurately.

6. Plane-Wave Impedance Fields

For the technical consistency in having one single kind of test apply over the entire radio-frequency spectrum, it would be desirable to use a plane-wave source at low frequencies since it is required at high frequencies. Even more important than technical consistency is the desirability of being able to determine from such tests effective electrical parameters, such as conductivity and permeability, for the shielded enclosure under test. From these effective parameters, it might be possible to calculate the performance of the shielded enclosure for an incident wave of any other impedance.

An attempt was made to create a plane wave at a frequency of 15 kc by sending a uniform current through a "planar" surface of hardware mesh (8 x 8 wires to the inch) approximately 12 feet x 8 feet in extent. Measurements indicated reasonably uniform magnetic field distribution over planes parallel to the current sheet and within several feet of it, except for locations within approximately 0.5 to 1.5 feet of the edges of the sheet. Electric field measurements were also performed, but the readings were disappointingly small. In other words, the wave impedance was far less than that of a plane wave.

Re-examination of the theoretical basis for such a source indicates that a uniform current should produce a uniform plane wave provided (and this point is not illuminated in earlier writings) that the uniform current sheet has the same impedance as free space, a condition not satisfied by the metallic surface of the test source.

Several suggestions have been made for overcoming this experimental difficulty. One is that current might be fed through a grid of high-resistance wires in order to permit setting up on adequate electric field at their surfaces. Another is that a plane wave might be generated synthetically be setting up the electric and magnetic fields separately. The uniform current sheet could be used to generate the magnetic field and a pair of parallel plates could be excited by a high potential to generate the electric field.

A decision whether to pursue these approaches will depend upon a forthcoming evaluation of the practical utility of such measurements.

C. Measurements at Mid-Frequencies

1. Introduction

The presence of standing waves in a shielded enclosure at or near the resonant frequencies reduces its shielding effectiveness, since an impinging electromagnetic field can generate fields inside the enclosure that are much larger than the plane wave theory would predict if there were no resonances. Furthermore, the field intensity inside can vary over wide limits inside the room because the Q of the shielded enclosure, considered as a cavity, is high. The performance of any electrical equipment placed inside the enclosures, at points where the field intensity is high because of resonance, can be affected in an unfavorable manner.

The shielded enclosure also has an influence on the impedance of a half-wave dipole antenna which is usually employed to measure its effectiveness at these frequencies, and makes it appear more reactive inside the room than it is outside.

The presence of standing waves and the change of antenna impedance makes any measurements taken at these (resonant) frequencies questionable, unless some knowledge is available about the behavior of the rom at these frequencies. The behavior at the resonant frequencies cannot be predicted from the known behavior of the enclosure at either low or high frequencies. Therefore, it is believed that a test should be established at or near its natural resonant frequencies.

2. The Shielded Enclosure as a Rectangular Cavitity

Any region bounded by conducting walls, within which resonant electromagnetic fields may exist in the form of standing waves, constitutes a cavity resonator. A cavity resonator may have an infinite number of resonant frequencies. Resonance in a rectangular cavity occurs when

$$(19) \qquad C = n\frac{\lambda_g}{2}$$

where:

c = length of the cavity resonator

λ_g = the guide wavelength of resonator, and n is an integer.

The shielded enclosure will act as a cavity resonator at its natural frequencies, f_{mnp}, given by[1]

$$(20) \quad f_{mnp} = \frac{c_o}{2}\sqrt{\left(\frac{m}{a}\right)^2 + \left(\frac{n}{b}\right)^2 + \left(\frac{p}{c}\right)^2}$$

where, as shown in Figure 12,

a = width = 1.94 meters for the room under test

b = height = 2.25 meters " " " " "

c = length = 3.00 meters " " " " "

and where no two of the integers m, n and p may be zero simultaneously.

* Reference (2), p. 533.

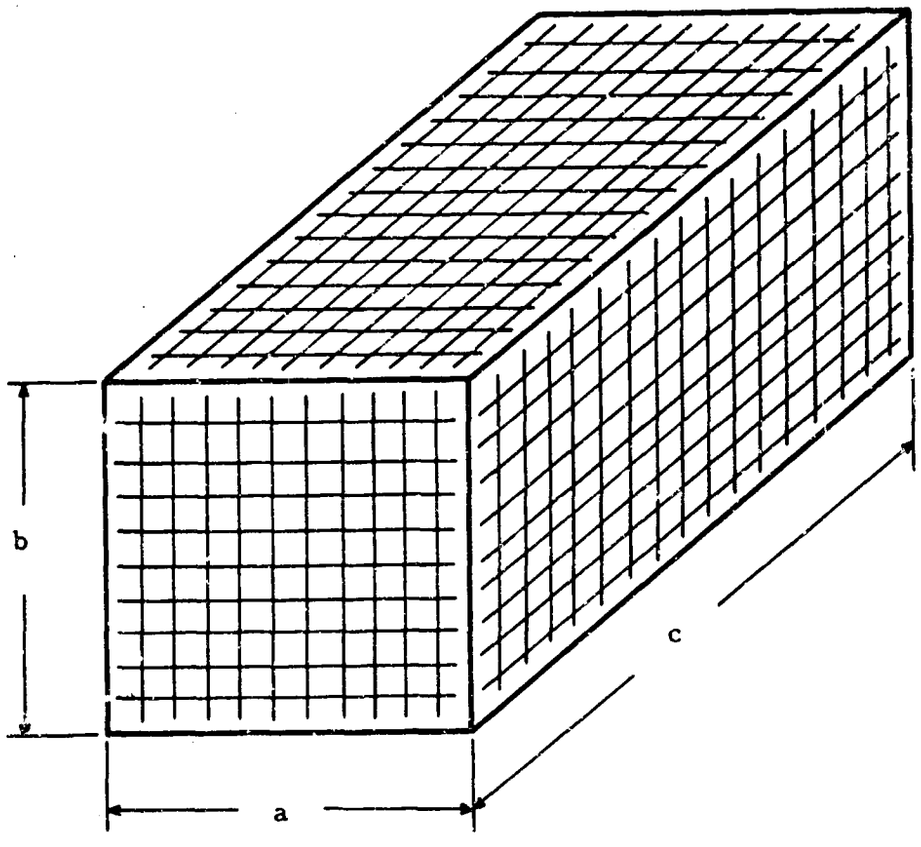

FIG. 12 - SHIELDED ENCLOSURE CONSIDERED AS A CAVITY

Some of the lowest resonant frequencies of the enclosure under test are

f_{110} = 102 mc	f_{011} = 83.4 mc	f_{210} = 167 mc	f_{112} = 143 mc
f_{101} = 92 mc	f_{111} = 114 mc	f_{120} = 155 mc	f_{122} = 184 mc
f_{221} = 210 mc	f_{322} = 332 mc	f_{233} = 323 mc	etc.

3. Experimental Results

a. Measurement of Resonant Frequencies

Attempts were made to measure experimentally the resonant frequencies of a cell-type copper-screened enclosure. In order to check the lowest group of frequencies around 100 mc, the TM_{011} mode was excited as shown in Figure 13. The two loops were made from RG-58/U cable with the shielding but not the insulation removed. The linear length of the loops was 18 inches. The room showed a resonance at 84 Mc which agrees with the predicted value.

The loops were replaced by short "monopoles" 6 inches long made from the same cable (see Figure 14). The monopoles were placed in the middle of the ab wall and perpendicular to it. This type of probe will excite TM modes, in a waveguide of cross section ab. Resonances were observed at 101.6, 215, and 322 mc. These are the TM_{110} TM_{221} and TM_{232} modes, respectively.

The resonances are confined to a very narrow bandwidth and are difficult to locate if not calculated before hand. The Q of the cavity is of the order of 540 at 215 Mc and follows the expected frequency variation, (the Q is lower at low frequencies and higher at high frequencies). The Q at f_o was measured by observing the bandwidth Δf (at the 3 db points) and calculating the Q from the formula

$$(10) \qquad Q = \frac{f_o}{\Delta f}$$

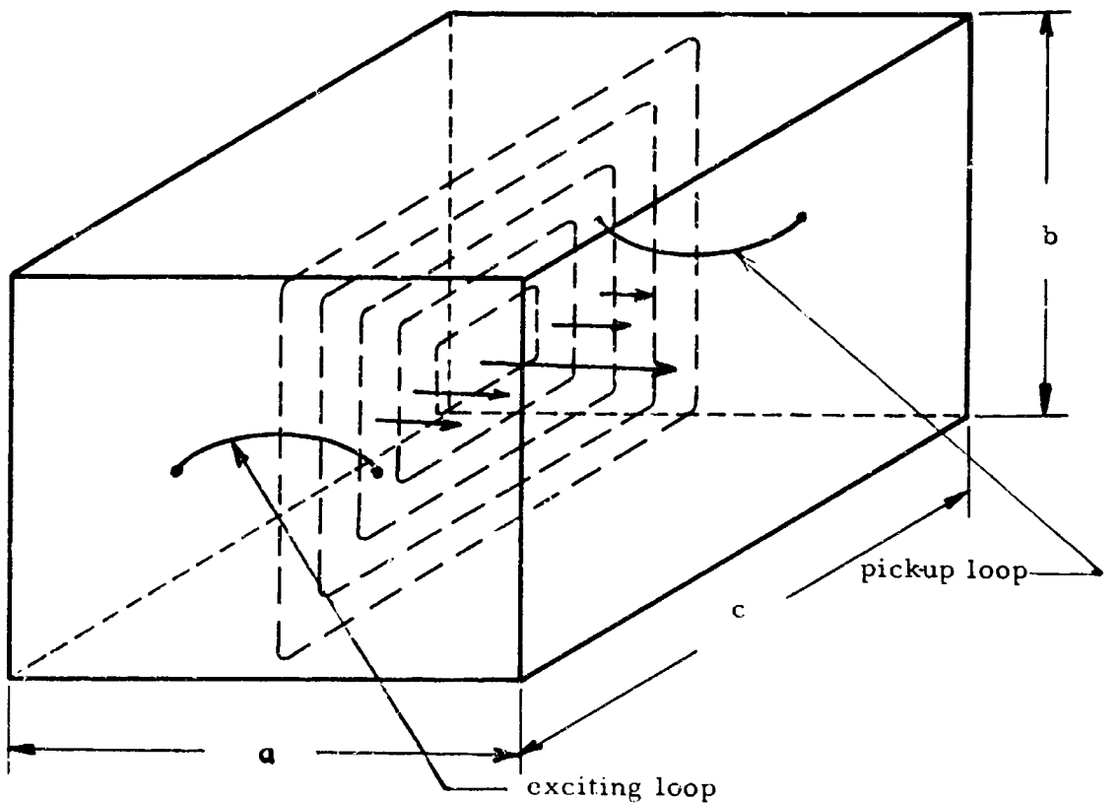

FIG. 13 - EXCITATION OF THE TM_{011} MODE

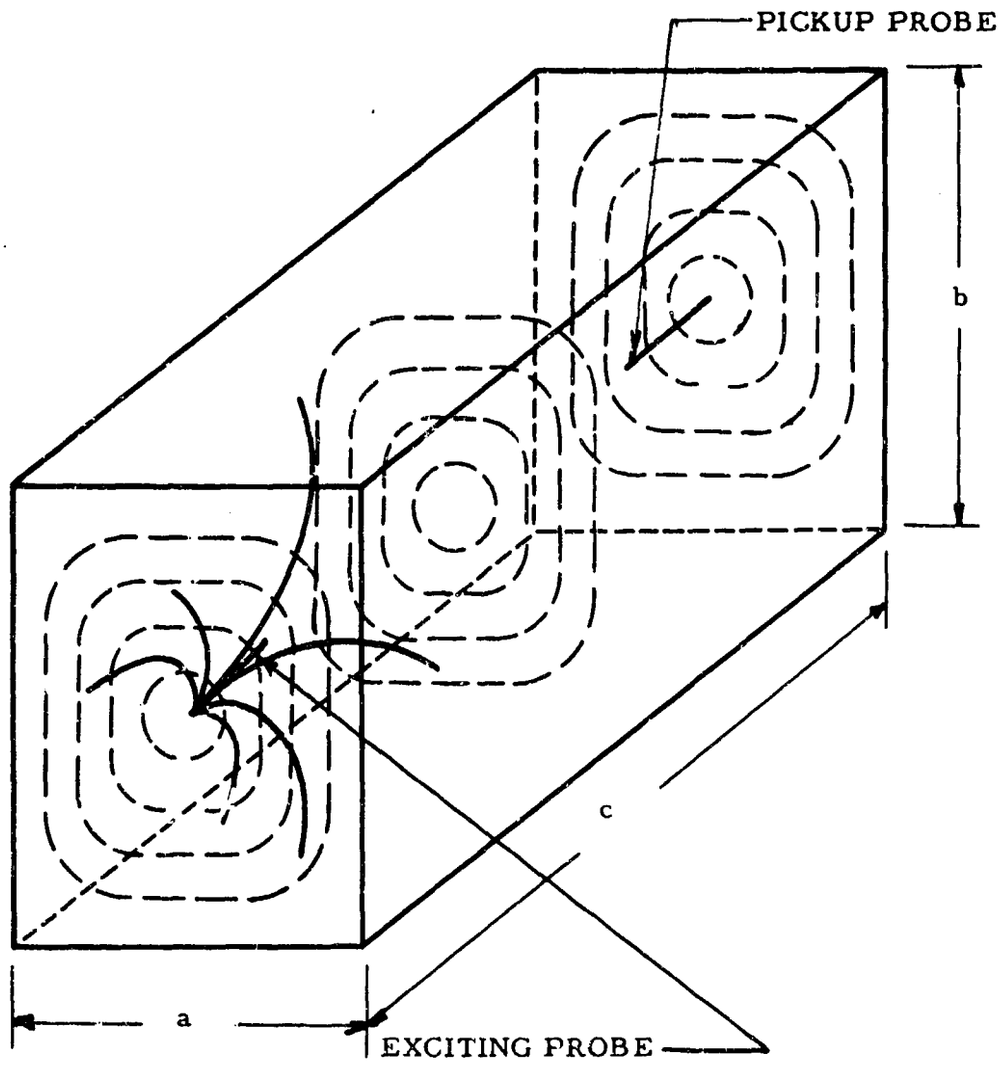

FIG. 14 - EXCITATION OF THE TM_{111} MODE

b. Effect of Absorbing Materials on Standing Waves

The magnitude of the standing waves in the screen room at the resonant frequency of 215 mc was measured. This was done by measuring the relative de-coupling between the two 6-inch short monopole antennas when placed, both inside and outside the shielded enclosure. The setup of Figure 15 depicts the method used in measuring the relative de-coupling. The signal generator was first connected to the detector through the pads and the voltage in the detector was recorded as V_1. The cavity (shielded enclosure) was then inserted between the pads and the voltage in the detector recorded as V_2. The de-coupling is then given as,

$$D = 20 \log \frac{V_2}{V_1} \tag{21}$$

At the resonant frequency of 215 mc, the de-coupling was -23 db. The antennas were taken outside the shielded enclosure, placed the same distance apart, and backed by 48-inch square copper plates acting as "ground planes" to simulate the sides of the shielded enclosure. At the same frequency the de-coupling was -40 db.

This test shows that since the coupling of the antennas is weaker outside, then there must be large fields residing in the shielded enclosure at the resonant frequencies. To verify this statement, lossy material was placed around the lower portion of the walls of the shielded enclosure covering a strip about two feet high. The coupling between the two antennas was reduced by 8.0 db.

The tests to determine the resonant frequencies experimentally were performed in order to obtain (1) some knowledge of the magnitudes of

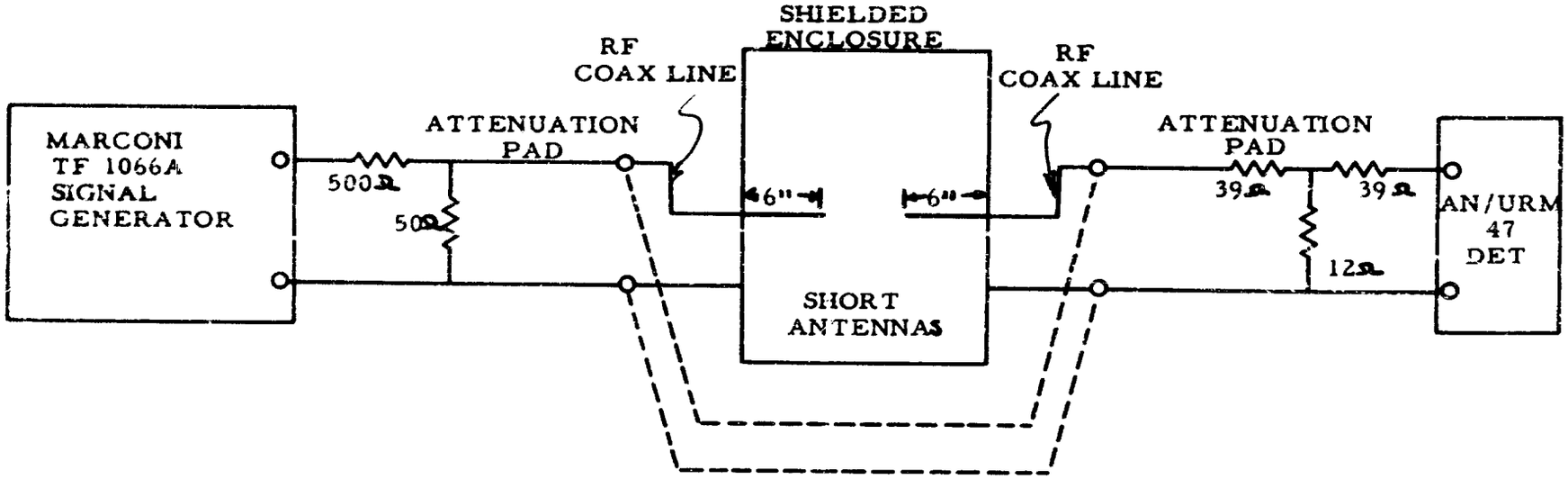

FIG. 15 - EXPERIMENTAL SET-UP FOR MEASUREMENT OF THE STANDING WAVES AT MID FREQUENCIES

the standing waves that are present within the shielded enclosure in the neighborhood of these resonant frequencies and (2) the amount of coupling of these fields to a dipole antenna.

4. Effects on Impedance of a Dipole

At the mid-frequencies, it is more convenient to use half-wave resonant dipoles for measuring the fields. The change in radiation impedance of such dipoles (both half-wave and electrically short) when in and out the shielded enclosure was measured with a Hewlett-Packard VHF Bridge. Tests were run at enclosure resonant frequencies and off resonant frequencies, namely at 83.4 mc, 150 mc and 215 mc. The test results indicate that the impedance of a half-wave, resonant-dipole antenna changes appreciably when placed inside the shielded enclosure and when rotated inside the enclosure. The change is more pronounced at the resonant frequencies of the enclosure. The change of impedance is not as great when the antenna is between a quarter and an eighth wavelength. The quantitative results of the tests are summarized in the table which appears on the next page.

D. High-Frequency Tests

1. Introduction

The electrical parameters ρ, μ, and ϵ of shielding materials change with frequency. Since the reflection and attenuation losses, and therefore the shielding effectiveness, depend on these parameters, a test of the performance of the shielded enclosure at high frequencies is necessary. The shielding effectiveness of an enclosure at microwave frequencies is high and is very much affected by both the spacing between shields (in the case of doubly shielded enclosures) and the spacing and size

TABLE I

IMPEDANCE OF DIPOLE ANTENNA OF DIFFERENT LENGTHS (ℓ) WHEN PLACED INSIDE AND OUTSIDE A RECTANGULAR SHIELDED ENCLOSURE

A. Measurements at the 83.4 mc. resonant frequency:

f (mc.)	Orientation of Antenna inside Shielded Enclosure	$\ell = \frac{\lambda}{2}$ Z_{in} ohms	$\ell = \frac{\lambda}{2}$ Z_{out} ohms	$\ell = \frac{\lambda}{4}$ Z_{in} ohms	$\ell = \frac{\lambda}{4}$ Z_{out} ohms	$\ell = \frac{\lambda}{8}$ Z_{in} ohms	$\ell = \frac{\lambda}{8}$ Z_{out} ohms
83.4	Longitudinally*	59/9°		459/45°		69/82°	
83.4	at 45°	128/-72°	27/-87°		542/37°		67/80°
83.4	Transversely**	196/-71°		310/57°		69/81°	

B. Measurements at the 215 mc. resonant frequency

f (mc)	Orientation of Antenna inside Shielded Enclosure	$\ell = \frac{\lambda}{2}$ Z_{in} ohms	$\ell = \frac{\lambda}{2}$ Z_{out} ohms	$\ell = \frac{\lambda}{4}$ Z_{in} ohms	$\ell = \frac{\lambda}{4}$ Z_{out} ohms
215	Longitudinally*	44/-52°	73/-16°	115/-67°	202/53°
215	Transversely	67/-72°	73/-16°	115/-67°	

C. Measurements 150 mc. off-resonant frequency

f (mc.)	Orientation Antenna ins Shielded Enclosure	$\ell = \frac{\lambda}{2}$ Z_{in} ohms	$\ell = \frac{\lambda}{2}$ Z_{out} ohms	$\ell = \frac{\lambda}{4}$ Z_{in} ohms	$\ell = \frac{\lambda}{4}$ Z_{in} hms	$\ell = \frac{\lambda}{8}$ Z_{in} ohms	$\ell = \frac{\lambda}{8}$ Z_{out} ohms
150	Longitudinally*	50/-77°		192/66°		93.8/79°	
150	Transversely**	320/3°	67/-18°	182/65°	136/66°	93.8/[illegible]°	71/78°

* Antenna oriented along dimension c of shielded enclosure.

** Antenna oriented along dimension a of enclosure.

of the perforations in the screening material. The space between shields can support high standing waves whenever the spacing is equal to $n\frac{\lambda}{2}$ where λ is the wavelength and n is an interger; this situation can bring about a 3-db decrease in shielding effectiveness below the value of a single screen wall.[1] During the next interval attempts will be made to find a relationship between the shielding effectiveness of perforated screening materials and corresponding wire meshes.

2. Hole-Dipole Theory

When a plane wave strikes a perforated conducting plane sheet of material, the radiation through the holes (perforations) can be described in terms of the fields from electric and magnetic dipoles within the holes.[2] The electric- and magnetic-dipole-moment strengths are proportional to the electric and magnetic fields of the incident plane wave that exists outside the hole. The constants of proportionality are called the polarizabilities and, for the case of simple geometries of holes, are given in the literature.[2, 3]

Consider a normally incident plane wave which has its electric and magnetic field components parallel to the perforated plane. Then only the magnetic-field component will contribute to the magnetic-dipole strength of the hole. The equivalent magnetic dipole lies on the plane of the hole and has a value

---

1 Reference (3), pp. 71-77

2 Reference (4), pp. 163-181

3 Reference (5), pp. 176-179

$$(22)\quad \mathcal{M} = -\frac{4}{3}\alpha^3 \mathcal{H}_0 = m_0 1_{H_0}$$

where

$\mathcal{M}$ = the magnetic moment

a = the radius of the hole

H_0 = the magnetic field of the incident plane wave of direction 1_{H_0}

Take the direction of $\mathcal{M}$ in the z direction. Then the fields at a point p(x, y, z) in front of a two-dimensional distribution of such magnetic dipoles will be given by[3]

$$(23)\quad E_\varphi(r,\theta,\varphi) = E_{\varphi_0}(r) F_{E0}(\theta,\varphi) F_x(\theta,\varphi) F_z(\theta,\varphi)$$

and

$$(24)\quad H_\theta(r,\theta,\varphi) = H_{\theta 0}(r) F_{H0}(\theta,\varphi) F_x(\theta,\varphi) F_z(\theta,\varphi)$$

where E_φ and H_θ are the total electric and magnetic fields at the point (r, θ, φ) due to N_x dipoles in the X- and N_z dipoles in the Z-direction, respectively.

In determining the total fields only the far-field component of each dipole is considered. Thus,

---

3 Reference (6), pp. 104-106

$$(25)\quad E_{\varphi_0}(r)\,F_{E0} = \frac{\beta}{4\pi}\sqrt{\frac{\mu}{\epsilon}}\,\frac{m_0}{r}\,e^{j(\omega t-\beta r)}\sin\theta$$

is the far-electric-field component due to a magnetic dipole of strength m_o at the origin and directed in the z direction,[1] and

$$(26)\quad H_{\theta 0}(r)\,F_{H0} = -\frac{\beta m_0}{4\pi r}\,e^{j(\omega t-\beta r)}\sin\theta$$

is the far-magnetic-field component due to a magnetic dipole of strength m_o at the origin and directed in the z direction.[2] Here $\beta = \frac{2\pi}{\lambda} = \frac{w}{c}$.

$F_x(\theta, \phi)$ and $F_Z(\theta, \phi)$ are form factors which modify the fields due to N_x and N_z dipoles in the X- and Z-directions, respectively.

Since a plane wave is incident on the perforated plane, all magnetic dipoles induced in the holes have the same magnitude and phase. Thus, from reference (6), pp. 104-106

$$(27)\quad F_x(\theta,\varphi) = e^{jN_x\beta a_x\sin\theta\cos\varphi}\left[\frac{\sin\left(\frac{N_x+1}{2}\beta a_x\sin\theta\cos\varphi\right)}{\sin\left(\frac{\beta a_x}{2}\sin\theta\cos\varphi\right)}\right]$$

and

$$(28)\quad F_z(\theta,\varphi) = e^{jN_z\beta a_z\cos\theta}\left[\frac{\sin\left(\frac{N_z+1}{2}\beta a_z\cos\theta\right)}{\sin\left(\frac{\beta a_z}{2}\cos\theta\right)}\right]$$

---

1 Reference (6), p. 95

2 Ibid. p. 96

where a_x and a_z are the separation between dipoles in the x and z directions, respectively, as shown in Figure 16.

For the purpose of our measurements, let $\theta = 90° = \phi$, and r = y (see Figure 16). Then $\sin\theta = \sin\phi = 1$ and $\cos\theta = \cos\phi = 0$ and Equations (27) and (28) become

$$(29)\quad F_x = N_x + 1 \qquad (30)\quad F_z = N_z + 1$$

respectively.

Since we work in free space

$$(31)\quad \beta = \frac{2\pi}{\lambda} \quad \text{and} \quad (32)\quad \sqrt{\frac{\mu}{\epsilon}} = \sqrt{\frac{\mu_0}{\epsilon_0}} = 120\pi$$

where $\lambda_0 = \frac{c}{f}$ and c is the velocity of light in free space.

To simplify calculations let

$$(33)\quad N_x = N_z = N$$

Equations (23) and (24) then become

$$(34)\quad E_\phi(y, 90°, 90°) = \frac{120\pi^2}{\lambda_0^2}\frac{m_0}{y}(N+1)^2 e^{j(\omega t - \frac{2\pi}{\lambda_0} y)}$$

and

$$(35)\quad H_\theta(y, 90°, 90°) = \frac{\pi}{\lambda_0^2}\frac{m_0}{y}(N+1)^2 e^{j(\omega t - \frac{2\pi}{\lambda_0} y)}$$

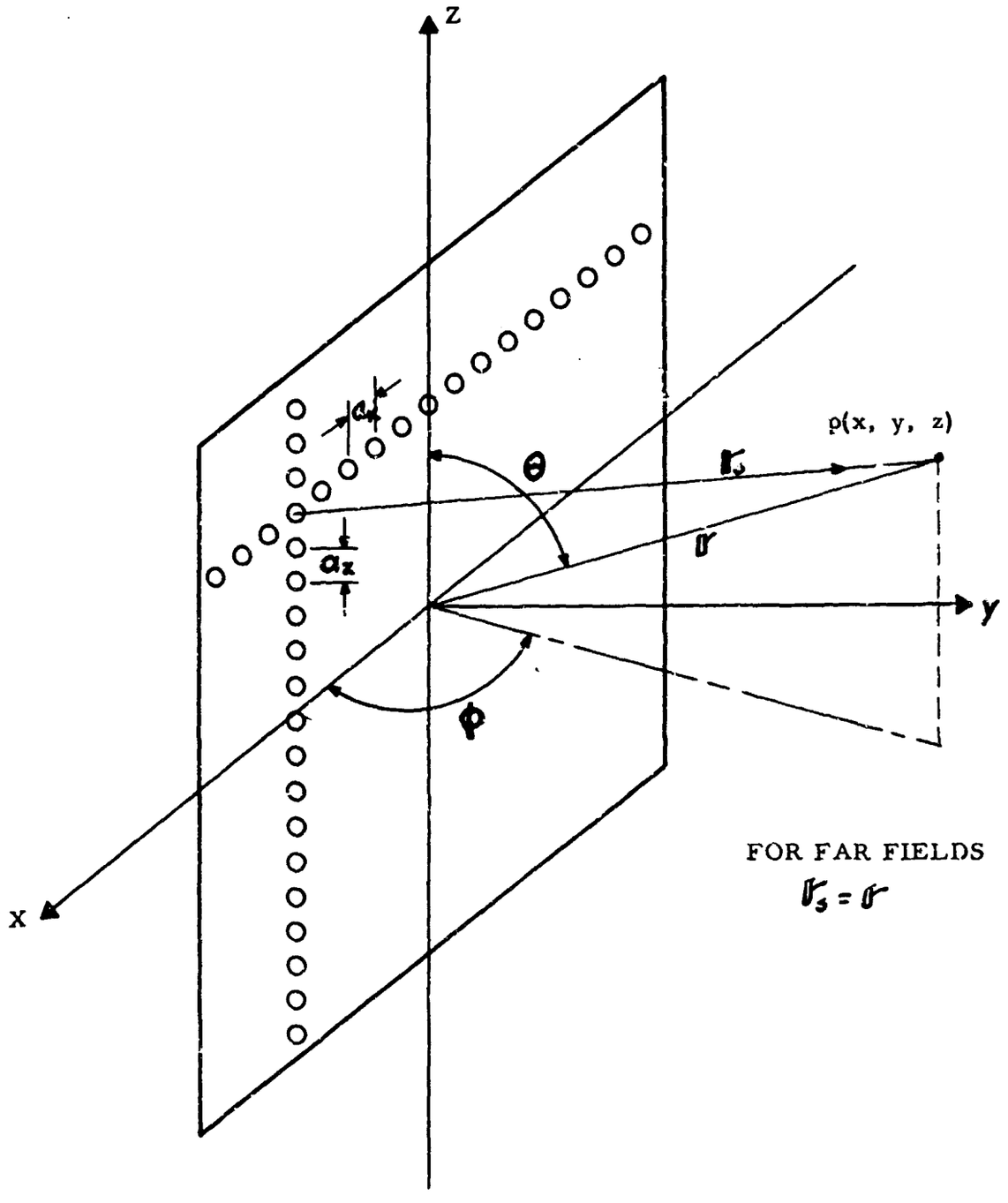

FIG. 16 - TWO DIMENSIONAL DISTRIBUTION OF DIPOLES

Equations (34) and (35) constitute the electric and magnetic fields of plane-wave traveling away from the screen and thus constitute the wave transmitted through the holes.

It is planned that a given area of a thin conducting sheet will be perforated, placed on a false door of the shielded enclosure, and illuminated with a plane wave. The radiation inside the shielded enclosure will be measured. In order to prevent leaking, the unused plane material and side panels will be covered with absorbing material. Measurements will be performed also on single layer and multi-layer wire mesh screens and a correlation will be sought between the shielding effectiveness of the perforated materials and the wire mesh materials.

3. Experimental Results

During this quarterly period, tests were initiated for the measurement of shielding effectiveness of screening materials and a screened room at the high end of a frequency range, e.g., 10,000 Mc. The source consists of an AN/APS-25 radar, the output of which is directed by means of a rectangular horn onto the screening material under test.

Variation of the reflection coefficient of the horn with distance from a plane sheet of conducting (screening) material was measured with a ratio meter, as shown in Figure 17, at 9.375 kmc. This test was performed to determine (1) how close a distance a horn can be placed to a shielding material (with good reflecting characteristics) before its radiation pattern is appreciably changed, and (2) the amount of reflected energy going back into the horn. Table II gives the results of the tests.

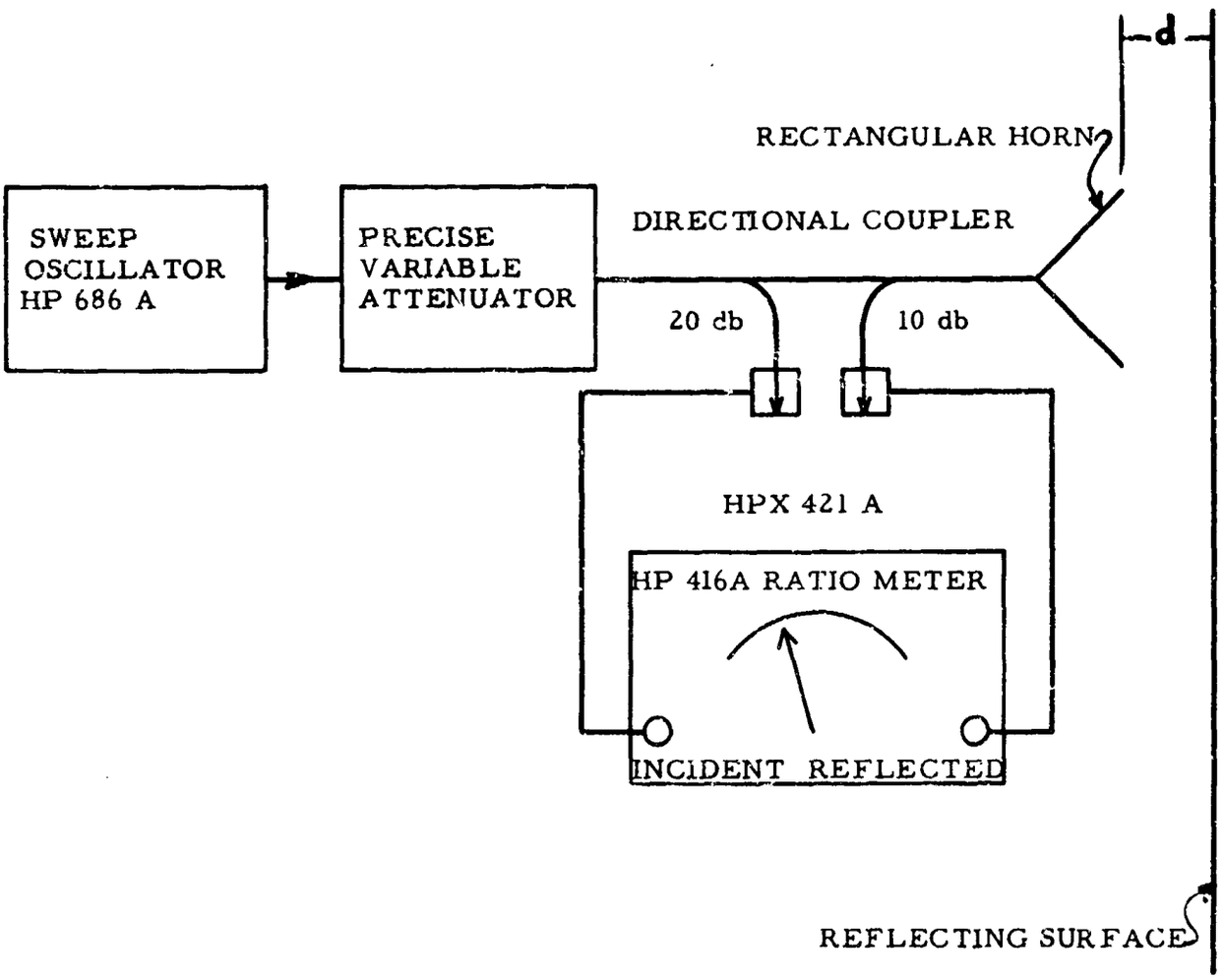

FIG. 17 - EXPERIMENTAL SET-UP FOR MEASURING THE REFLECTION COEFFICIENT OF A HORN ANTENNA

TABLE II

DETERMINATION OF P OF A HORN AT X-BAND WHEN IT ILLUMINATES A PLANE SHEET OF SCREENING MATERIAL

A. Solid Copper Sheet 4' x 4' x 1/32"

d (cm)	5	10	15	20	25	30	50	130	210
P_{max}	.58	.40	.25	.23	.22	.20	.17	.12	.10
P_{min}	.28	.13	.06	.03	.02	.02	.03	.08	.06

B. One Panel of Screening Room

d (cm)	25	30	60	90	120
P	.09	.09	.08	.15	.06

The maximum and minimum values of the reflection coeficient, P, in the case of the solid copper sheet, were obtained by tilting the copper sheet forward to backward from its vertical position. Pressing the screen room material so as to distort its plane surface changes the reflecting coefficient from three to five times the undisturbed value. These facts indicate that the distance of the horn from the reflecting surface should be kept at least 15 to 20 wavelengths so that uniform illumination and least scattering in the off-normal direction to the surface will result. The energy source will also be protected from excessive amounts of reflected power.

Initially, the coupling between two rectangular horns when the screen room was and was not intervening was measured. The insertion

loss of the screen room at 9.375 kmc was found to be an average* value of about 80 db. As a detector, an AN/URM-42 instrument, an IM-52/URM-17 Radio-Interference/Field-Intensity Meter with a TN-131/APR-9 tuning head, was used. More precise tests on the screen room and on different screening materials will be performed during the next quarterly interval.

Attempts will also be made to investigate the behavior of joints at microwave frequencies.

E. Coaxial Testing Device

1. Introduction

In the Second Quarterly Progress Report it was indicated that a section of coaxial transmission line could be used to measure the shielding effectiveness of materials to plane-waves. A lamina of the material is inserted in the line as a barrier extending from the inner to the outer coaxial conductors and perpendicular to them, as in Figure 18. The justification for assuming that the barrier will respond to the TEM mode in a coaxial waveguide, in the same manner that it would to a plane wave, was given in the Second Quarterly Progress Report.

2. Field Theory Equivalent Circuit

It is of interest to examine the analogy between the coaxial waveguide and the transmission line. Below a given frequency determined by the dimensions of the coaxial waveguide only the TEM mode will propagate.

---

* Maximum and minimum values of attenuation are obtained by changing the separation distance of the two screens corresponding to a separation between shields of $(2n+1)\frac{\lambda}{4}$ and $2n\frac{\lambda}{2}$, respectively, where n is an integer.

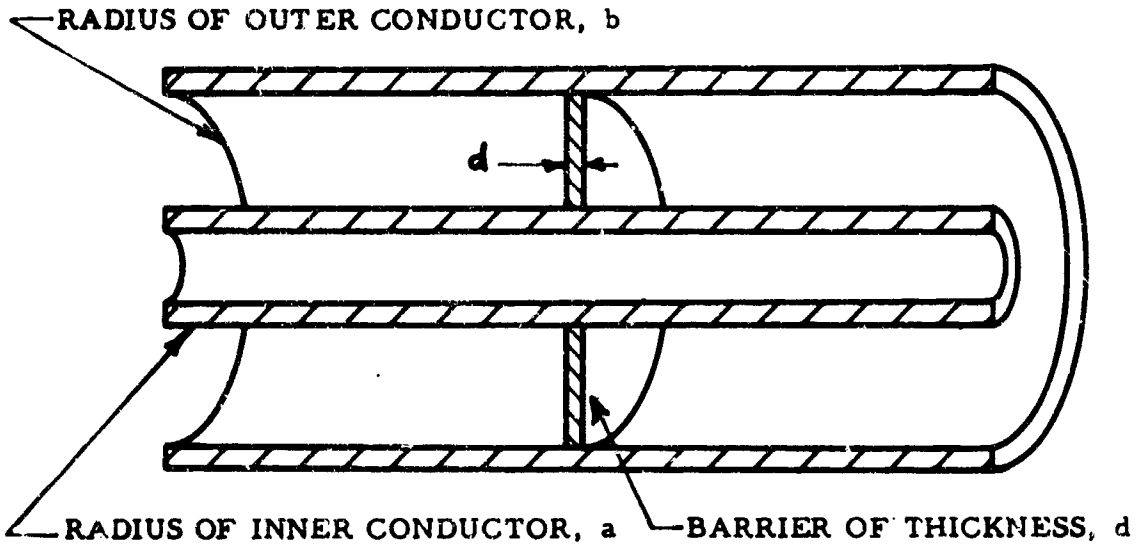

FIG. 18 - CROSS-SECTIONAL VIEW OF COAXIAL TEST DEVICE

When wall losses are negligible, the field equations are given by

$$(36)\quad \frac{\partial H_\varphi}{\partial z} = -(\sigma + j\omega\epsilon) E_\rho = -\gamma H_\varphi$$

$$(37)\quad \frac{\partial E_\rho}{\partial z} = -j\omega\mu H_\varphi = -\gamma E_\rho$$

where

E_ρ is the radial electric field of the TEM mode, and

H_φ is the circumferential magnetic field.

The variation of the fields along the length of the waveguide and in time is given by $e^{jwt - \gamma z}$, where $\gamma^2 = jw\mu(\sigma + jw\epsilon)$ has its usual significance.

The relationship between the field quantities (the electric and magnetic fields) and the voltage across the current along the line can be obtained from Maxwell's equations. Now

$$(38)\quad \oint \mathbf{H} \cdot d\mathbf{l} = I(z) = H_\varphi(\rho, z) 2\pi\rho$$

where $I(z)$ is the current along the transmission line. From this it follows that

$$(39)\quad H_\varphi(\rho, z) = \frac{I(z)}{2\pi\rho}$$

The impedance of the TEM mode is $jw\mu/\gamma$. Hence,

$$(40)\quad \frac{E_\rho}{H_\varphi} = \frac{j\omega\mu}{\gamma} \ .$$

For the radial electric field, the solution is

$$(41)\quad E_\rho = \frac{j\omega\mu}{\gamma} H_\varphi = \frac{j\omega\mu}{\gamma} \frac{I(z)}{2\pi\rho} \ ,$$

The voltage drop across the waveguide is the line integral of the radial electric field,

$$(42)\quad V(z) = \int_a^b E_\rho \, d\rho = \frac{j\omega\mu}{\gamma} \frac{\ln\frac{b}{a}}{2\pi} I(z) \ .$$

Insert (39) and (42) in (36) and (37) to yield

$$(43)\quad \frac{\partial V}{\partial z} = -j\omega\mu \frac{\ln\frac{b}{a}}{2\pi} I(z)$$

and

$$(44)\quad \frac{\partial I}{\partial z} = -(\sigma + j\omega\epsilon) \frac{2\pi}{\ln\frac{b}{a}} V(z)$$

These are the transmission line equations and the series impedance and shunt admittance per unit length of the line are given by

$$(45)\quad Z = j\omega\mu \frac{\ln\frac{b}{a}}{2\pi} \qquad (46)\quad Y = (\sigma + j\omega\epsilon) \frac{2\pi}{\ln\frac{b}{a}}$$

respectively.

As previously indicated, the coaxial testing device consists of a section of coaxial transmission line containing a lamina of the material under test. The lamina extends from the inner to the outer conductor and is perpendicular to them. The extremely short piece of line containing the lamina may be considered as a short piece of coaxial transmission line whose interior is filled with the metal under test. For most metals $\omega\epsilon \ll \sigma$. Consequently, the line containing the metal can be considered as a piece of transmission line whose per unit-length impedance and admittance are given by,

$$(47)\quad Z = \frac{j\omega\mu \ln\frac{b}{a}}{2\pi} \qquad (48)\quad Y = \frac{\sigma 2\pi}{\ln\frac{b}{a}}$$

The coaxial testing device can, therefore, be considered as a section of air-filled transmission line in which is inserted a section of transmission line whose length is equal to the thickness of the lamina and whose impedance and admittance per unit length are given by (47) and (48). The characteristic impedance of the air-filled line is denoted $\overline{\overline{Z}}$ and is equal to 60 ln b/a. Using this result, the impedance and admittance per unit length of the metal filled line are given by:

$$(49)\quad Z = \frac{\mu\overline{\overline{Z}}\omega j}{120\pi} \qquad (50)\quad Y = \frac{120\pi\sigma}{\overline{\overline{Z}}}\ .$$

The impedance and admittance of the barrier which is of thickness d can thus be given as

$$(51)\quad Z_b = \frac{\mu\overline{\overline{Z}}d}{120\pi}j\omega \qquad (52)\quad Y_b = \frac{120\pi d\sigma}{\overline{\overline{Z}}}\ .$$

From a circuit theory viewpoint, Z_β can be considered to be due to an inductance L_β equal to $\frac{\mu E d}{120\pi}$ and Y_β as due to a shunt resistance given by R_S equal to $\frac{E}{120\pi d\sigma}$. Since $\sigma = 1/\rho$, where ρ is the bulk resistivity, the shunt resistance can also be given by R_S equal $\frac{E\rho}{120\pi d}$. The equivalent circuit for device is illustrated in Figure 19.

3. Circuit-Theory Equivalent Circuit

At the lower frequencies, it is useful to consider the coaxial testing device from a circuit theory viewpoint. The circuit equivalent is given in Figure 20. This circuit follows from transmission line theory when R_g is the characteristic impedance of the line. To develop the ideas of reflection and attenuation loss for this circuit, the discussion will be phrased in terms of "waves".

The circuit equations are

$$(53)\quad V_{oc} = (R_g + R_s + j\omega L) I_1 - R_s I_2$$

$$(54)\quad 0 = -R_s I_1 + (R_g + R_s + j\omega L) I_2$$

The voltage at the input terminals to the T-section, V_1, is given by

$$(55)\quad V_1 = V_{oc} - I_1 R_g$$

and since from (53) and (54)

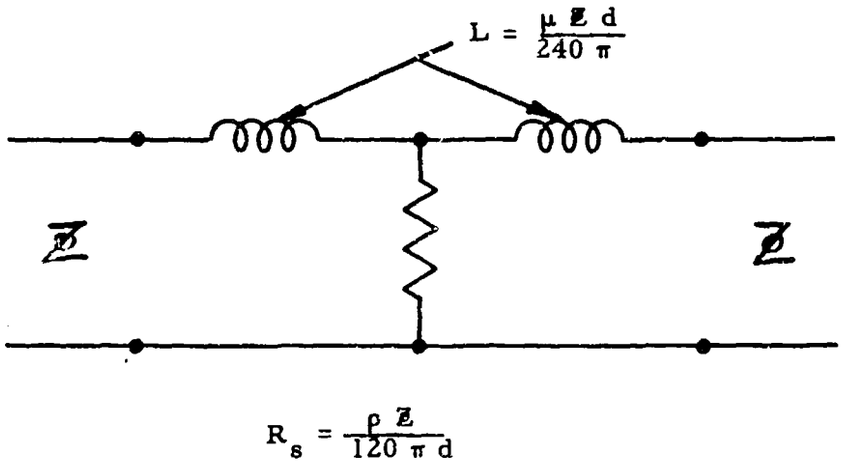

FIG. 19 - TRANSMISSION-LINE EQUIVALENT TO COAXIAL TESTING DEVICE

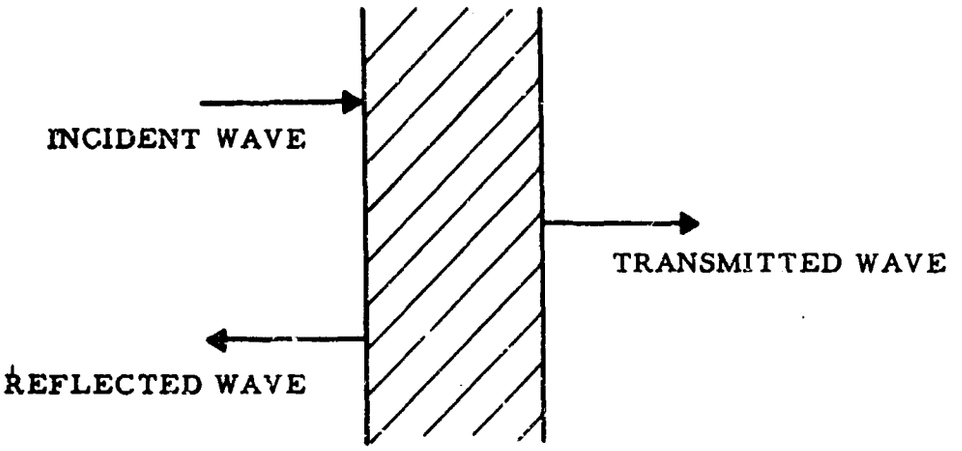

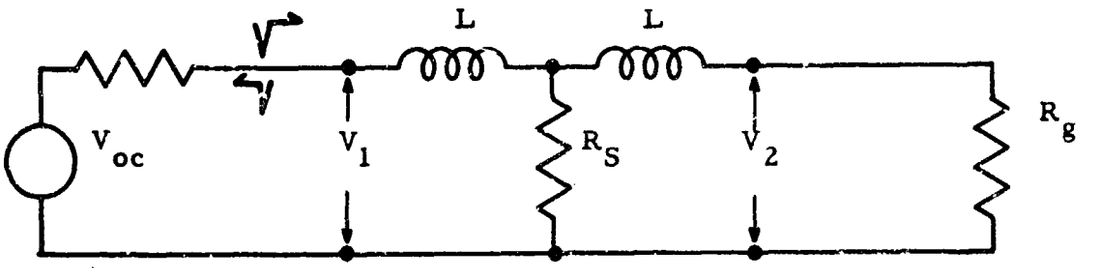

INCIDENT WAVE $\Longleftrightarrow$ V^+

REFLECTED WAVE $\Longleftrightarrow$ V^-

TRANSMITTED WAVE V_2

	ATTENUATION LOSS	REFLECTION LOSS
FIRST ORDER APPROXIMATION	$AL^{(1)} = \dfrac{R_S + j\omega L}{R_S}$	$RL^{(1)} = \dfrac{R_g}{2(R_S + j\omega L)}$
SECOND ORDER APPROXIMATION	$AL^{(2)} = \dfrac{R_S + j\omega L}{R_S}$	$RL^{(2)} = \dfrac{R_g + 2(R_S + j\omega L)}{2(R_S + j\omega L)}$

FIG. 20 - CIRCUIT THEORY AND TRANSMISSION LINE EQUIVALENCE

$$(56)\quad I_1 = \frac{V_{oc}(R_g + R_s + j\omega L)}{(R_g + R_s + j\omega L)^2 - R_s^2}$$

it follows that

$$(57)\quad V_1 = V_{oc}\left\{\frac{R_g(R_s + j\omega L) + 2R_s j\omega L - \omega^2 L^2}{(R_g + R_s + j\omega L)^2 - R_s^2}\right\}$$

The voltage at V_1 can be considered as the sum of two voltage waves,

$$(58)\quad V_1 = \overrightarrow{V} + \overleftarrow{V}$$

where $\overrightarrow{V}$ is the forward traveling or incident voltage wave and $\overleftarrow{V}$ is the backward traveling or reflected voltage wave. The forward traveling voltage wave $\overrightarrow{V}$ is evidently given by

$$(59)\quad \overrightarrow{V} = \frac{V_{oc}}{2}$$

since it is that voltage which the generator would deliver to a matched load. The generator here is considered to be a zero impedance source, having an open circuit voltage V_{oc}, in series with an impedance R_g. Using equations (57), (58) and (59) it follows that the reflected voltage wave is

$$(60)\quad \overleftarrow{V} = -V_{oc}\left\{\frac{R_g^2 + \omega^2 L^2 - 2R_s j\omega L}{2R_g - 2\omega^2 L^2 + 4R_g R_s + 4R_g j\omega L + 4R_s j\omega L}\right\}$$

It is useful, for simplicity, to establish two levels of approximation,

First order - neglect ωL and R_s as compared to R_g

Second order - neglect $\omega^2 L^2$ and R_s^2 as compared to R_g^2.

The first and second order approximations for V_1, $\overleftarrow{V}$, and $\overrightarrow{V}$ are thus,

1st order approximation*

$$(61)\quad V_1^{(1)} = V_{oc}\,\frac{R_s + j\omega L}{R_g}$$

$$(62)\quad \overrightarrow{V}^{(1)} = \frac{V_{oc}}{2}$$

$$(63)\quad \overleftarrow{V}^{(1)} = -\frac{V_{oc}}{2}$$

2nd order approximation

$$(64)\quad V_1^{(2)} = V_{oc}\,\frac{R_s + j\omega L}{R_g + 2(R_s + j\omega L)}$$

$$(65)\quad \overrightarrow{V}^{(1)} = \frac{V_{oc}}{2}$$

$$(66)\quad \overleftarrow{V}^{(1)} = -\frac{V_{oc}}{2}\left\{\frac{R_g}{R_g + 2(R_s + j\omega L)}\right\}$$

---

* The sum $\overrightarrow{V}^{(1)} + \overleftarrow{V}^{(1)}$ is not equal to $V_1^{(1)}$ because of the approximations involved.

These equations describe that part of $V_{oc}/2$ which is lost be reflection to a first and second order of approximation. The voltage V_2 which appears across the output of the T-section can be considered to be the transmitted wave and is given by $I_2 R_g$ or since

$$(67) \quad I_2 = \frac{R_s V_{oc}}{(R_g + R_s + j\omega L)^2 - R_s^2}$$

then

$$(68) \quad \vec{V_2} = \frac{R_s R_g V_{oc}}{(R_g + R_s + j\omega L)^2 - R_s^2} = V_2 .$$

The first and second order approximations for $\vec{V}_2$ are

$$(69) \quad \vec{V}_2^{(1)} = V_{oc} \frac{R_s}{R_g}$$

$$(70) \quad \vec{V}_1^{(2)} = V_{oc} \frac{R_s}{R_g + 2(R_s + j\omega L)} ,$$

It is evident that from equations (59), (62), (69) and (70) that

$$(71) \quad \vec{V}_2^{(1)} = V_1^{(1)} \frac{R_s}{R_s + j\omega L}$$

$$(72) \quad \vec{V}_2^{(2)} = V_1^{(2)} \frac{R_s}{R_s + j\omega L}$$

The results can be interpreted as follows. The generator delivers a forward traveling voltage wave which travels to the T-section

where a wave, $\overleftarrow{V}$, is reflected back to the generator. The voltage V_1 can be thought of as a wave which passes into the T-section, is attenuated, and passes out of the T-section toward the load R_g. Since R_g is a matched load, the wave out of the T-section is not reflected at R_g.

The transmitted wave represented by $\overrightarrow{V}_2$ can be given as the product of the incident wave $\overrightarrow{V}$ and two factors.

$$(73)\quad \overrightarrow{V}_2^{(1)} = V_1^{(1)} \frac{R_s}{R_s + j\omega L} = \frac{V_{oc}}{2} \frac{2(R_s + j\omega L)}{R_g} \cdot \frac{R_s}{(R_s + j\omega L)}$$

or, since $\overrightarrow{V} = \frac{V_{oc}}{2}$

$$(74)\quad \overrightarrow{V}_2^{(1)} = \overrightarrow{V} \frac{2(R_s + j\omega L)}{R_g} \frac{R_s}{R_s + j\omega L} .$$

The corresponding second order approximation is

$$(75)\quad \overrightarrow{V}_2^{(2)} = \overrightarrow{V} \left[\frac{2(R_s + j\omega L)}{R_g + 2(R_s + j\omega L)}\right]\left[\frac{R_s}{(R_s + j\omega L)}\right] .$$

The reciprocal of the first term represents the reflection loss RL, the reciprocal of the second term represents the attenuation loss, AL.

$$(76)\quad RL^{(1)} = \frac{R_g}{2(R_s + j\omega L)} \qquad (77)\quad AL^{(1)} = \frac{R_s + j\omega L}{R_s}$$

$$(78)\quad RL^{(2)} = \frac{R_g + 2(R_s + j\omega L)}{2(R_s + j\omega L)} \qquad (79)\quad AL^{(2)} = \frac{R_s + j\omega L}{R_s}$$

These equations indicate, as expected, that the reflection loss decreases with L while the attenuation loss increases with L. If the reflection and attenuation loss are expressed in terms of db, then the total loss is their sum.

Further insight into the equivalence of the circuit analog can be obtained by recalling the values for L and R_s

$$(80)\quad L = \frac{\mu \mathcal{Z} d}{240\pi} \qquad (81)\quad R_s = \frac{\rho \mathcal{Z}}{120\pi d}$$

and letting R_g equal $\mathcal{Z}$. The formulas for the reflection and attenuation loss take the form,

$$(82)\quad RL^{(1)} = \frac{60\pi}{\frac{\rho}{d} + j\omega\mu\frac{d}{2}} \qquad (83)\quad AL^{(1)} = \frac{\frac{\rho}{d} + j\omega\mu\frac{d}{2}}{\frac{\rho}{d}}$$

$$(84)\quad RL^{(2)} = \frac{60\pi + \frac{\rho}{d} + j\omega\mu\frac{d}{2}}{\frac{\rho}{d} + j\omega\mu\frac{d}{2}} \qquad (85)\quad AL^{(2)} = \frac{\frac{\rho}{d} + j\omega\mu\frac{d}{2}}{\frac{\rho}{d}}$$

Since the total loss is the product of reflection and attenuation loss, it is evident that

$$(86)\quad \vec{V}_2^{(1)} = \frac{\vec{V}}{RL^{(1)} AL^{(1)}} = \frac{\rho}{60\pi d}\vec{V}$$

$$(87)\quad \vec{V}_2^{(2)} = \frac{\vec{V}}{RL^{(2)} AL^{(2)}} = \frac{\rho/d}{60\pi + \frac{\rho}{d} + j\omega\mu\frac{d}{2}}\vec{V}.$$

Thus, the insertion loss, when viewed from the waveguide, transmission line, or circuit theory viewpoint, indicates (as it necessarily must) that

the measured insertion loss is only a function of the constitutive parameters of the barrier and its thickness.

4. Experimental Evaluation

Experimental verification of the coaxial testing device has been delayed for two reasons: (1) difficulty has been experienced in reducing the contact resistance between the coaxial structure and the sample barrier, and (2) the Rollins Signal Generator used as a source developed two faults which required correction.

The method of using the coaxial device is shown in Figure 21. The device is constructed of standard 1-5/8 inch coaxial cable having a 50-ohm characteristic impedance. Transitions are used to couple the coaxial device to RG-8 cable. Since the measurements are most easily interpreted when the device is fed by a 50-ohm source and terminated in a 50-ohm load, the device is isolated from the Rollins Signal Generator and Field Intensity Meter by 50-ohm T-pads having an insertion loss of about 15 db. The use of the pads reduces the overall sensitivity of the device by 30 db. It may be necessary to reduce the isolation of the T-pads in order to achieve higher sensitivity at the expense of a slight reduction in accuracy.

As previously indicated, one of the primary problems involved in developing the coaxial test device has been that of reducing contact resistance. From a circuit theory viewpoint the device can be regarded as one for measuring very low impedances (the resistance and inductance of the barrier). When such measurements are made, either contact resistance must be kept low compared to the impedance of the sample or it must be located in the circuit in such a manner that it does not influence

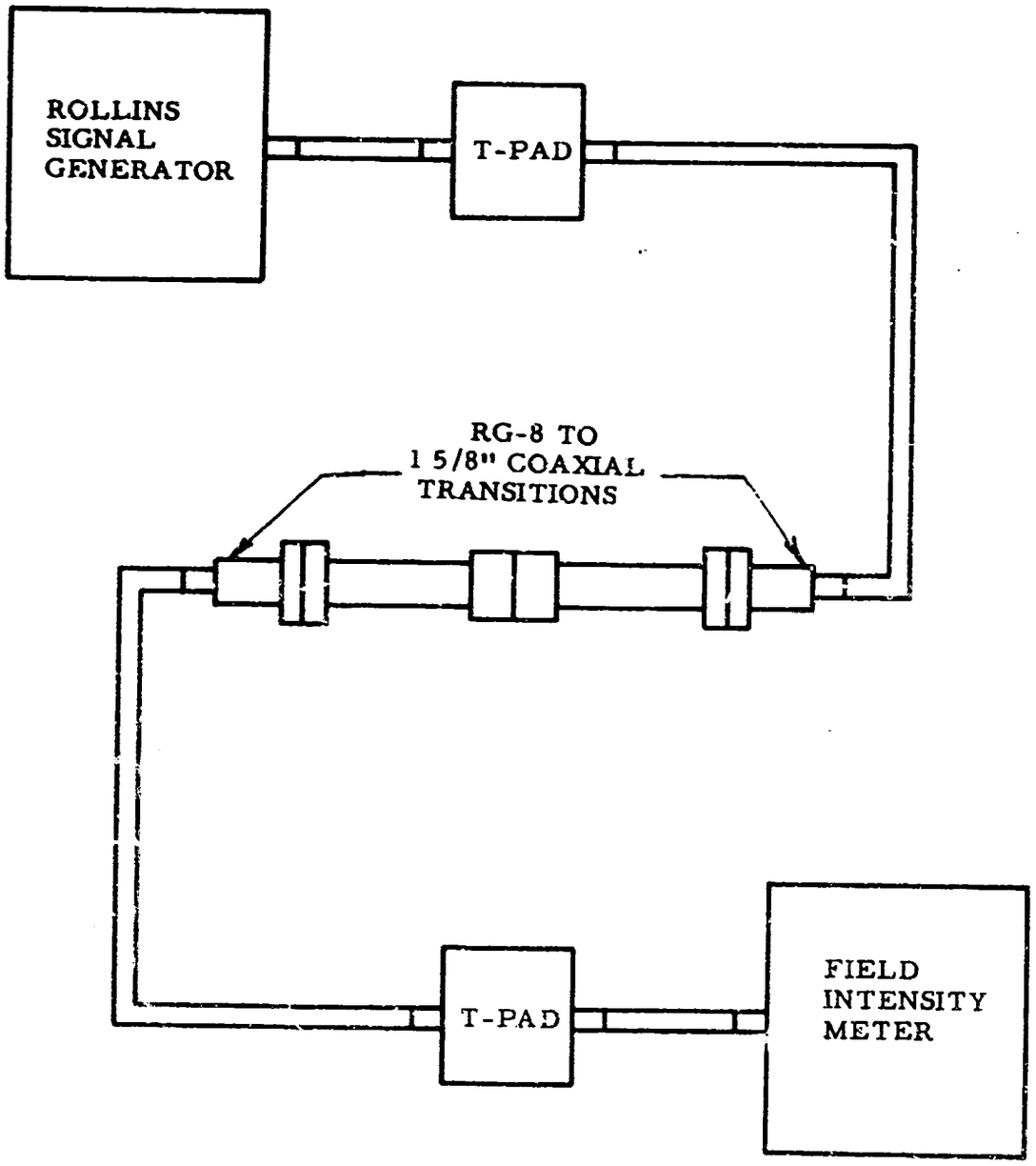

FIG. 21 - ARRANGEMENT FOR COAXIAL TESTING DEVICE

the measurement. The latter approach is used, for example, in the Kelvin Bridge.

The construction of that part of the device which holds the sample is shown in Figure 22. Originally, the outer threaded collars and inner threaded collar and stud were made of brass. A circuit representation of the device is as indicated in Figure 23. Because the contact resistance and sample resistance are very small, the generator drives a current through the sample which is determined almost by the internal impedance of the generator. Consequently, a voltage drop appears across the contact resistances and sample which in turn causes a current to flow through the load. The magnitude of this current is determined almost entirely by the load resistance. The voltage drop across the load is measured by the voltmeter.

Since the contact resistance may be large compared to the sample resistance, it represents a very serious source of error. Soldering the sample to the coaxial device can help to reduce contact resistance but gives rise to practical problems in assembling the device.

It is believed that the problem of contact resistance can be circumvented by constructing the threaded collars and stud of insulating material. The contact resistance in the desired current paths (Figure 22) will still be present however, the voltage drop across this resistance will not appear across the voltmeter and will not influence the measurement. The use of an insulating stud and collar will remove the undesired current paths so that no voltage drop will result from such currents which previously passed through the contact resistance between the lamina and the load side of the line. The device has been modified so that the collar is

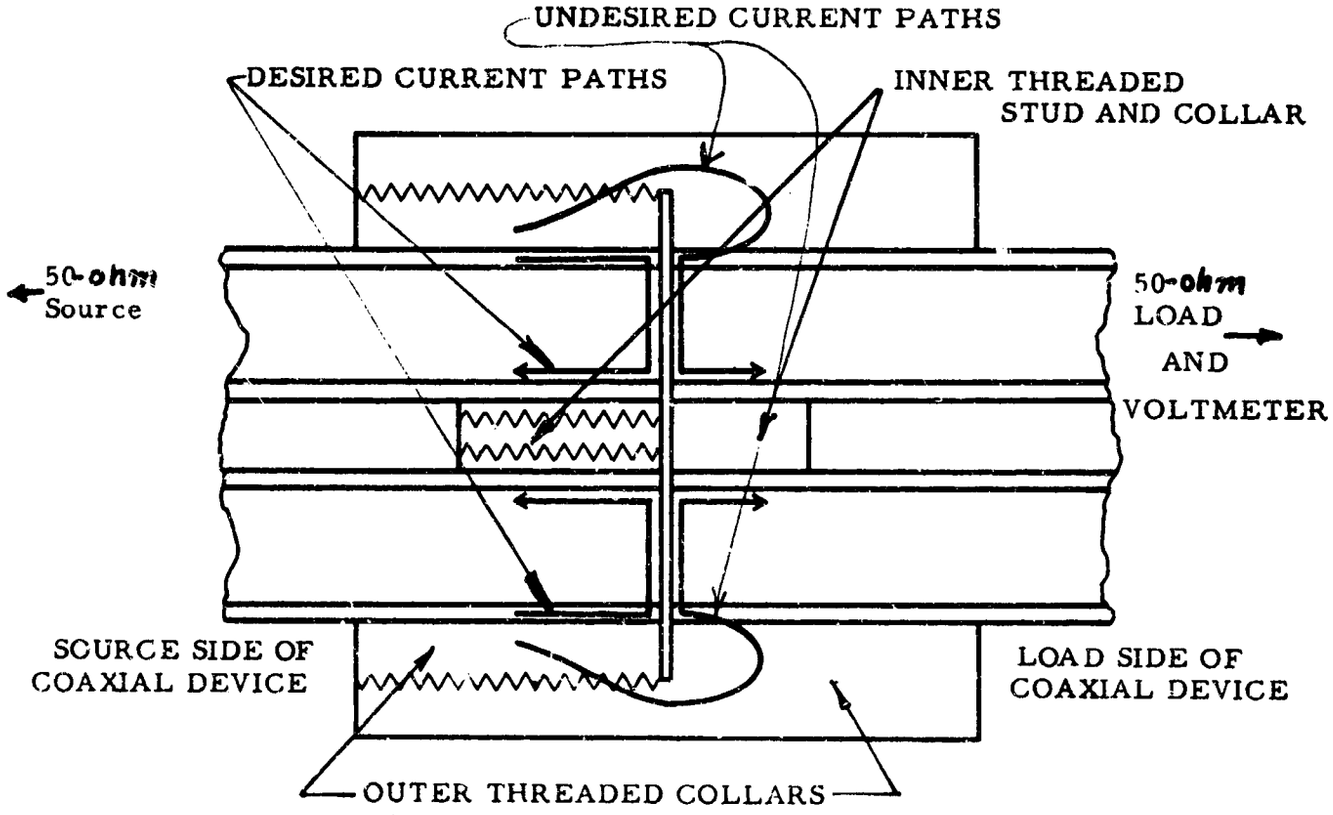

FIG. 22 - CONSTRUCTION OF SAMPLE-RECEIVING PORTION OF COAXIAL DEVICE

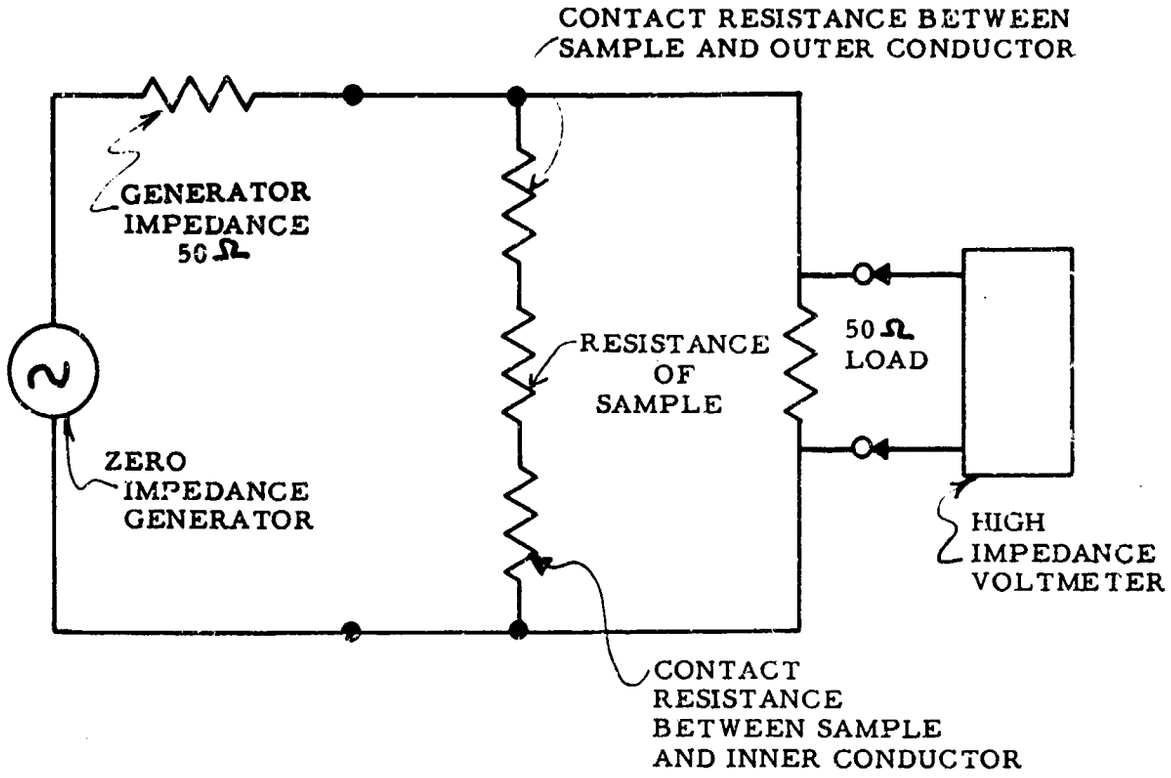

a. WITH BRASS COLLARS AND STUD

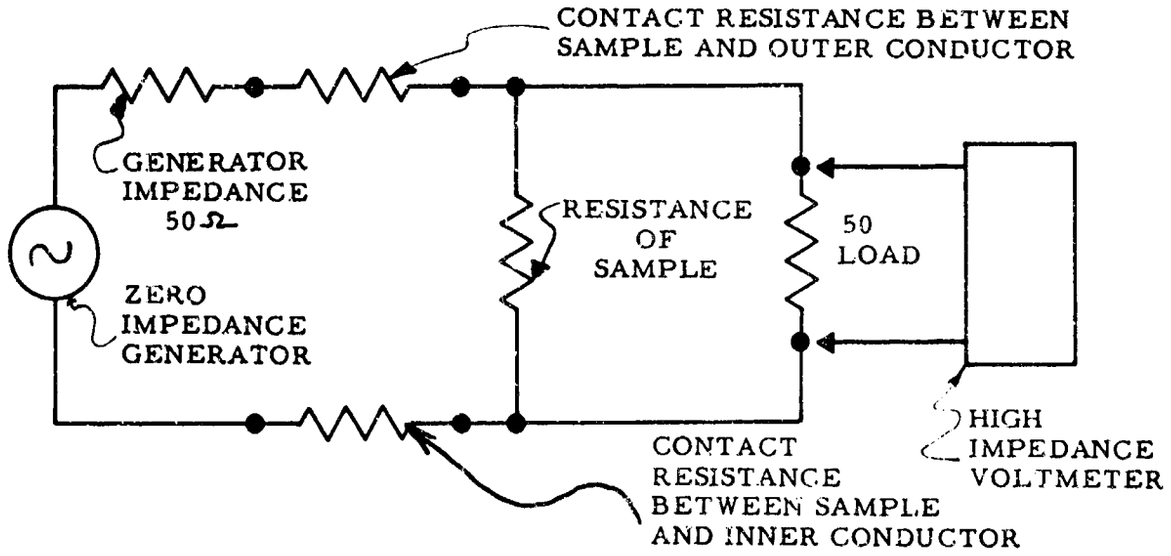

b. WITH INSULATING COLLARS AND STUD

FIG. 23 - CIRCUIT EQUIVALENTS FOR COAXIAL DEVICE

made of linen impregnated plastic and the stud of nylon. The modifications were completed just prior to the writing of this report and initial tests indicate that the problem of contact resistance has been resolved.

F. Project Performance and Schedule Chart

The scheduling of the program of research is shown in Figure 24. The open areas represent planned effort while the shaded area represent completed work. The financial status of the project is as follows:

For the period ending 28 February 1959*

Original money allocated for research	$37,672
Total expenditures	21,426
Total commitments	462
Balance available for research	15,784

It is anticipated that the expenditures for March 1959 will be approximately $3,400.

IV. CONCLUSIONS

1. The advantages of using a large loop to immerse the enclosure in a low-impedance, low-frequency field are that a pick-up loop in the center of the enclosure can then be used to provide an overall indication of performance, and a small pick-up loop can be employed to explore for local defects.

---

* Cost sheets for March 1959 are not available until April 20, 1959.

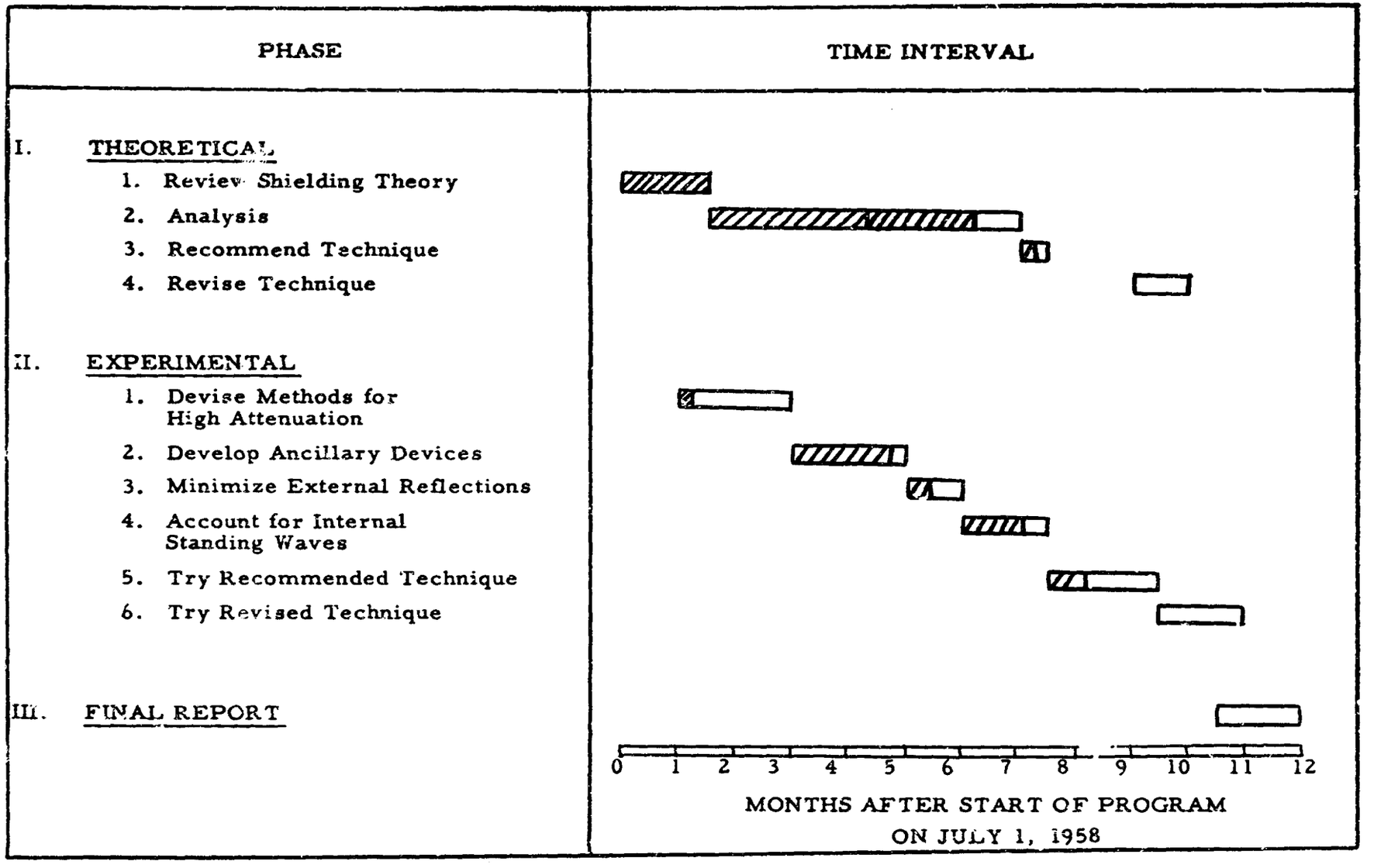

FIGURE 24 PROJECT SCHEDULE CHART

2. The inverse frequency formula for the reduction of coupling between two coaxial loops due to a conducting sheet does not appear to fit the experimental data. The data is fitted fairly well by a formula which gives the reduction as being proportional to an exponential in which the exponent if (a) negative, (b) proportional to the thickness of the material, and (c) proportional to the square root of the frequency.

3. Measurements of the resonant frequencies of an enclosure indicate that they can be predicted with a high level of accuracy by use of the formula for the resonant frequencies of a rectangular cavity. Q's of the order of 500 have been observed; however, these can be reduced significantly by placing absorbers within the enclosure.

4. The impedance of a dipole, when it is inside and outside of an enclosure, has been measured and it has been found that the difference in impedance is not significant if the dipole is electrically short (about one-eight wavelength).

5. Initial tests indicate that it will be possible to measure the effectiveness of a double-wall screened enclosure in the neighborhood of 10 kilomegacycles using and AN/URM-17 as a detector, horns as antennas, and a pulsed radar as a source. Preliminary results indicate a penetration of about -80 db for this type enclosure. The penetration has been found to be dependent upon the spacing between the two sheets of screen material, as predicted by theory.

6. The use of an insulating collar and stud in the coaxial testing device causes it to function more nearly like a Kelvin Bridge and initial tests indicate that this modification will minimize the effects of contact resistance.

V. PROGRAM FOR NEXT INTERVAL

During the next quarterly period, effort will be expended on the following aspects of the program.

1. Experimental investigation of the coaxial device for evaluating shielding material will be continued.
2. Investigation of the nature of standing waves inside shielded enclosures at the resonant frequencies will be continued.
3. Measurement of the shielding effectiveness of the enclosure for plane waves in the neighborhood of various resonant frequencies will be initiated.
4. Investigation of the possibility of reducing the Q of the shielding enclosure by appropriately lining the enclosure interior with absorbing materials will be conducted.
5. An attempt to develop practical formulas for perforated and screening materials, to give the intrinsic impedance and thickness of an equivalent solid metal barrier that would provide the same shielding effectiveness as the screening materials, will be made.
6. Tentative Testing Standards for the measurement of attenuation of shielded enclosures will be set up, and trial runs will be made to test the recommended technique.

VI. LOGBOOKS

Data obtained on this project are contained in Logbooks C 8375, C 8724, and C 8836.

Respectfully submitted,

ARMOUR RESEARCH FOUNDATION
of Illinois Institute of Technology

L. C. Peach

L. C. Peach, Research Engineer

R B Schulz for HMS

H. M. Sachs, Assistant Supervisor
Electronic Interference

APPROVED:

S. I Cohn

S. I. Cohn, Assistant Manager
Electrical Engineering Research